

# CHALMERS



## Tyre modelling for rolling resistance

BHARAT MOHAN REDROUTHU

SIDHARTH DAS

Department of Applied Mechanics  
*Division of Vehicle Engineering and Autonomous System*  
Vehicle Dynamics Group  
CHALMERS UNIVERSITY OF TECHNOLOGY  
Göteborg, Sweden 2014  
Master's thesis 2014:24



MASTER'S THESIS IN AUTOMOTIVE ENGINEERING

# Tyre modelling for rolling resistance

BHARAT MOHAN REDROUTHU

SIDHARTH DAS

Department of Applied Mechanics  
*Division of Vehicle Engineering and Autonomous System*  
Vehicle Dynamics Group  
CHALMERS UNIVERSITY OF TECHNOLOGY  
Göteborg, Sweden 2014

# Tyre modelling for rolling resistance

BHARAT MOHAN REDROUTHU

SIDHARTH DAS

© BHARAT MOHAN REDROUTHU, SIDHARTH DAS, 2014

Master's Thesis 2014:24

ISSN 1652-8557

Department of Applied Mechanics

Division of Vehicle Engineering and Autonomous System

Chalmers University of Technology

SE-412 96 Göteborg

Sweden

Telephone: + 46 (0)31-772 1000

# **Tyre modelling for rolling resistance**

BHARAT MOHAN REDROUTHU

SIDHARTH DAS

Chalmers University of Technology

Göteborg, Sweden 2014

Report No. 2014:24

## **ABSTRACT**

Increased efficiency in road vehicle is a demand in today's society in the view of rising fuel cost and emission regulation. An important source for losses in road vehicles is tyre rolling resistance. For tyres with rolling resistance coefficient of 0.012, the fuel consumption due to tyre rolling resistance losses can amount to 20% - 30% of total consumption depending on the drive cycle, according to the study 'the tyre: rolling resistance and fuel savings' by Michelin, 2003. This study investigates mathematical models based on physical understanding and literature reviews of tyre rolling resistance phenomena. The work aims to develop a tyre model that explains the influence of tyre inflation pressure, tyre size, velocity and normal load on the rolling resistance coefficient. The model is based on free rolling condition without taking the longitudinal slip into account. The consideration of the model developed includes vertical tyre stiffness with geometrical belt constraint accounting for tyre vertical deflection and counter-deflection, tyre viscous and coulomb damping effect and rotational aerodynamic drag effect. The vertical stiffness model accounts for tyre geometry indirectly by means of constants in the model. The stiffness model and the simple lumped damping model together takes into account various hysteresis losses.

The tyre model developed for rolling resistance gives results which are in very good agreement with the experimental data. For example an 8.3% increase in tyre outer radius from 60 cm to 65 cm, the proposed model predicts a reduction of 4.8% in tyre rolling resistance coefficient compared to 5% suggested by experimental data. Furthermore, a change to low rolling resistance tyre in LeanNova's energy simulation model corresponds to a reduction in the average energy consumption by 3.8% for a NEDC run in an electric vehicle and a reduction of 1.3% in average fuel consumption for a NEDC run in a conventional vehicle. Through these findings and the proposed tyre model that calculates rolling resistance by taking a limited number of tyre parameters into consideration, a foundation for physical understanding of tyre rolling resistance phenomena is established.

**Keywords:** Rolling resistance, tyre model, physical model, belt model, tyre dimension, energy consumption



# Contents

1	INTRODUCTION	1
1.1	Background	1
1.2	Aim	1
1.2.1	Deliverables	2
1.3	Scope and Limitations	2
2	LITERATURE REVIEW	3
2.1	Understanding tyres	3
2.1.1	Construction of tyres	4
2.1.2	Mechanism of load carrying	6
2.1.3	Mechanism of road grip	7
2.1.4	Mechanism of Rolling Resistance	10
2.2	Influence of tyre parameters on rolling resistance	11
2.2.1	Influence of tyre size	11
2.2.2	Influence of tyre inflation pressure	14
2.2.3	Influence of normal load	15
2.2.4	Influence of longitudinal velocity	16
3	MODELLING	18
3.1	Basic Assumptions	18
3.2	Radial spring and damper distribution	18
3.3	Balloon model and stiffness	21
3.4	Constant Belt Model	23
3.5	Damping Model	25
3.6	Rotational aerodynamic drag	26
3.7	Combined Model	28
3.8	Final tuning coefficients and their significance	29
3.9	Simulink Block for energy simulation	30
4	RESULTS AND DISCUSSION	31
4.1	Influence of longitudinal velocity	31
4.2	Influence of tyre outer diameter	32
4.3	Influence of contact patch width	33
4.4	Influence of tyre inflation pressure	34
4.5	Influence of normal load	35
4.6	Energy simulation results	36
5	CONCLUSION AND FUTURE WORK	41

5.1	Conclusion	41
5.1.1	Combined Model	41
5.1.2	Energy simulations	42
5.2	Future Work	43
6	REFERENCES	44
	APPENDIX I	44



# Preface

In this research work, the influence of various tyre parameters on rolling resistance has been examined with emphasis on the parameters that influence the development of a new vehicle platform such as section width and outer radius. This thesis work was carried out from January 2014 to June 2014 under the supervision of Dr. Gunnar Olsson and Rudolf Brziak at LeanNova Engineering AB and Professor Bengt Jacobson at Chalmers University of Technology. This work should enable LeanNova to perform high-quality tyre selection processes related to vehicle platform development. The project is carried out partly at the Vehicle Engineering & Autonomous Systems (VEAS), Chalmers University of Technology, Sweden and partly at LeanNova Engineering AB, Sweden. The project is financed by LeanNova Engineering AB.

We would like to thank the supervisors, staff and PhD students in the research group of vehicle dynamics at Chalmers University of Technology and LeanNova Engineering AB for their time and guidance despite their hectic schedules and responsibilities. We would also like to extend our deepest gratitude to Zuzana Sabartova, PhD student at Chalmers for her valuable inputs in this thesis work.

Gothenburg, Sweden, June 2014

Bharat Mohan Redrouthu

Sidharth Das



# Notations

## Abbreviations

AEC	Average Energy Consumption
CoG	Centre of Gravity
EV	Electric Vehicle
ICE	Internal Combustion Engine
KN	Kilo Newton
KPa	Kilo Pascal
KWh	Kilo Watt Hour
LBs	Pounds
NEDC	New European Driving Cycle
Psi	Pounds per Square Inch
RR	Rolling Resistance Force
RRC	Rolling Resistance Coefficient

## Roman upper case letters

C	Elemental spring damping coefficient from balloon model
$C_c$	Coulomb damping coefficient
$C_d$	Aerodynamic drag coefficient
$C_{RR}$	Coefficient of rolling resistance
$C_v$	Viscous damping coefficient
D	Tyre outer diameter
F	Maximum frictional resistance force
$F_{AirDrag}$	Rotational aerodynamic drag
$F_s$	Sliding friction
$F_z$	Sum of spring and damper forces
$F_{RR}$	Rolling resistance force
K	elemental spring stiffness from balloon model
$K_z$	Vertical stiffness from constant belt model
L	Contact patch length
N	Normal Load
P	Tyre inflation pressure
R	Outer Radius
R	Equivalent reaction force in figure 2.12
T	Torque on wheel
$V_x$	Longitudinal velocity
W	Tyre width or section width
W	Watts

## Roman lower case letters

a	Deformed radius at middle of contact patch
e	Pressure centre offset
z	Vertical deformation of contact patch element
$\dot{z}$	Rate of Vertical deformation of contact patch element
x	Position of the element at the contact patch measured from the centre

### **Greek lower case letters**

$\theta$	Angle of element from centre line of contact patch
$\theta_{\max}$	Maximum angle of element from centre line of contact patch
$\omega$	Angular velocity of element in contact patch
$\mu$	Coefficient of static friction
$\mu_s$	Coefficient of sliding friction

# 1 Introduction

Global warming is a huge concern now and the transportation sector is the biggest contributor to greenhouse gases after electricity production [1]. In efforts to reduce the greenhouse emissions stricter emission targets are being set. With a current fleet average CO<sub>2</sub> emission target set at 130 g/km for cars in 2015 and a projected target of 95 g/km for 2021 set by the European commission for Europe, there is a huge amount of research in making green vehicles. Greenhouse emissions are directly proportional to fuel consumption; hence reducing fuel consumption will reduce CO<sub>2</sub> emissions. There are various ways of improving the fuel efficiency. Some of them include using better, more efficient powertrains, such as improved downsized engines, using hybrid vehicles, alternative fuels, or totally electric vehicles. Another area of focus is on reducing the road load. Road load is a force which opposes the movement of a vehicle. The main focus is on the forces acting on the car such as aerodynamic drag and rolling resistance.



**Figure 1.1 Implication of low rolling resistance tyres**

It has been found that rolling resistance can account for as much as 20% of all the losses in the vehicle and hence it is an important road load that needs to be reduced.

## 1.1 Background

The thesis work is initiated by Dr. Gunnar Olsson, Senior Engineer at LeanNova Engineering AB in Trollhättan, to better understand the influence of various parameters that can influence the tyre selection for a new passenger vehicle platform. There have been different opinions about the relation between rolling resistance of tyres and tyre parameters such as outer diameter and tyre width. To better understand the trends and to be able to select the right tyre for a new vehicle platform, there is a need to understand the rolling resistance dependence on various parameters such as width, outer radius, longitudinal velocity, normal load and inflation pressure.

Selection of the right tyre for a vehicle is very important, especially during development of a new platform. The chosen tyre parameters can affect the entire vehicle such as the height of the vehicle, the height of CoG, frontal area and width of the car apart from rolling resistance and various performance parameters such as acceleration, braking and cornering performance of the vehicle. Therefore, there is a need to fully understand the rolling resistance dependencies on some tyre parameters in order to be able to choose a good tyre size to enable a good total optimization of the car.

## 1.2 Aim

The aim of this Master Thesis is to develop a tyre model that calculates the rolling resistance based on input parameters such as size, geometry and tyre inflation pressure and operating conditions such as vertical load, torque and speed. The model should be based on physical understanding of the rolling resistance phenomena. This is to enable

a comparison between different tyres for choosing the best option that gives minimum rolling resistance for same traction requirement, at a given load and road condition.

### **1.2.1 Deliverables**

A tyre model that evaluates rolling resistance based on the input of different parameters of the tyre.

- Physical explanation of the rolling resistance dependence on each parameter
- Mathematical model calculating tyre rolling resistance.
- Simulink block for LeanNova energy simulation environment

## **1.3 Scope and Limitations**

A tyre is a very complicated component of the vehicle, impacting the vehicle performance and behaviour in several ways. There have been many models for tyres. Depending on the type of output required, the tyre has been modelled with respect to comfort, traction, noise and so on. In this study, a model is developed to understand some operational and design parameters of the tyre with respect to rolling resistance, while not considering few other design parameters such as tyre material, tread pattern, road types and temperature. They are considered beyond the scope of the thesis work due to limited time, information and knowledge of the subject. Furthermore, the tyre model applies to free rolling cases and does not include any torque application to wheels or longitudinal slip. This means the model does not calculate longitudinal stiffness and subsequent contribution to longitudinal force due to this. Hence the contribution to energy consumption values due to the longitudinal slip phenomenon is unaccounted for.

There are many assumptions in the thesis such as contact patch shape is assumed to be perfect rectangle; inflation pressure doesn't change with deflection, tyre material and tread pattern are kept constant; on a modern conventional passenger car tyre. Road type is fixed to hard, dry and flat surface. The model accounts for pneumatic tyre designs, however motorcycle tyres or round profile tyres are not considered in the study. Road type is assumed to be a hard dry surface. Temperature is assumed to be a constant, steady state parameter. While this may not be entirely true, it has been found from literature that they are reasonable approximations in the quest to initiate an understanding of the rolling resistance phenomenon. Due to limited time and resources, most of the tyre information has been taken from various research papers and correspondingly, most constants used have been obtained thereof.

## 2 Literature Review

In this section the contribution of rolling resistance to the total losses in a vehicle is discussed. In this respect, an understanding of the influence of various parameters on tyre rolling resistance coefficient and the conflict of reducing rolling resistance with vehicle requirements is also discussed.

The overall fuel consumption of a vehicle depends on many factors. They are generally of the following categories.

- Inertia losses dissipated during deceleration or downhill driving
- Aerodynamic drag on both vehicle body and wheels
- Rolling resistance
- Longitudinal slip

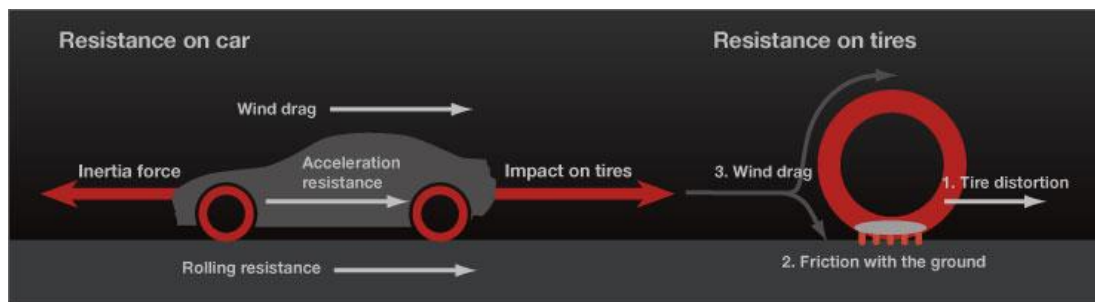


Figure 2.1: Resistance on a car [2]

The current trend of making more efficient vehicles has created a considerable interest in understanding rolling resistance and its dependence on various parameters so that the overall efficiency of the vehicle can be improved.

### 2.1 Understanding tyres

A tyre must perform a number of functions in a vehicle. It should cushion, dampen, assure good directional stability and provide long service life. But primary concern is the road holding quality such as being able to transmit strong longitudinal and lateral forces during acceleration, braking and cornering manoeuvres at different road conditions.

Due to the wide range of demands, optimising tyre design for certain characteristics can be often a compromise. Some of the characteristics to be considered while designing are shown figure 2.2.

## Conflicting goals in tyre development

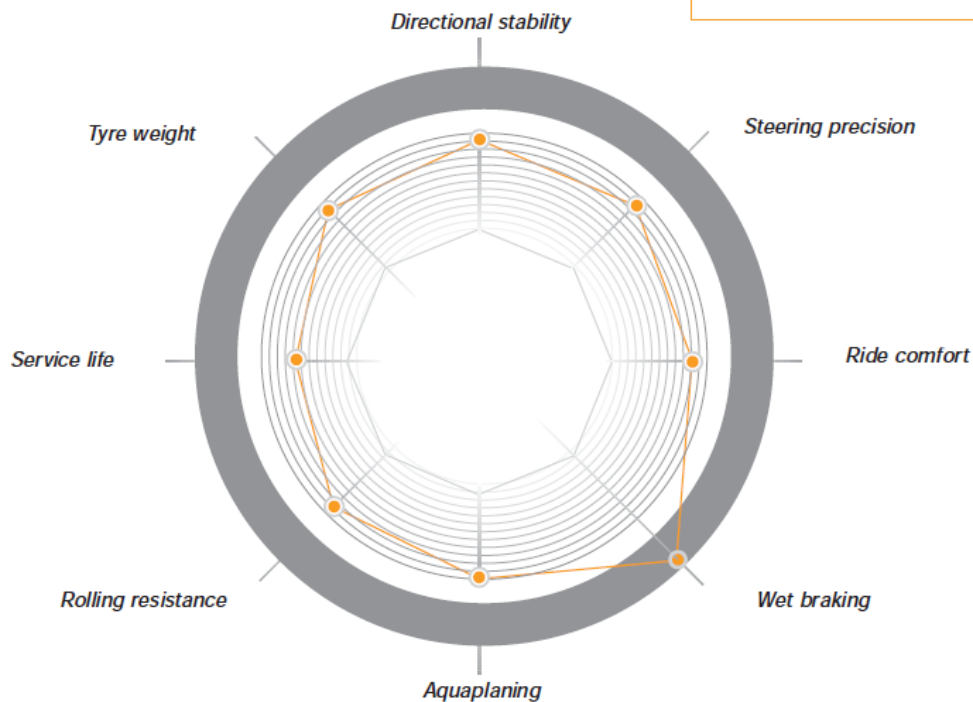


Figure 2.2: Conflicting goals in tyre development [3]

In addition to the goals shown above, there are few additional goals such as packaging, longitudinal traction, winter road grip, loose ground grip, etc.

There are some known ways of reducing rolling resistance. The most important and significant of them is the tread compound. When the tread compound is designed for rolling resistance, it compromises other performance characteristics like braking and acceleration capability, wet traction, aquaplaning and so on. To achieve a good road grip, the tread compound should have high-hysteresis. This phenomenon is explained in section 2.1.3. However, hysteresis which is responsible for good grip also increases rolling resistance. Hence there is always a trade-off. Another way of reducing rolling resistance is by changing the size and dimension of the tyre structure. The influence of tyre size is discussed in section 2.2.1.

### 2.1.1 Construction of tyres

Currently tyres can be divided into two major types of construction.

- Cross ply
- Radial ply



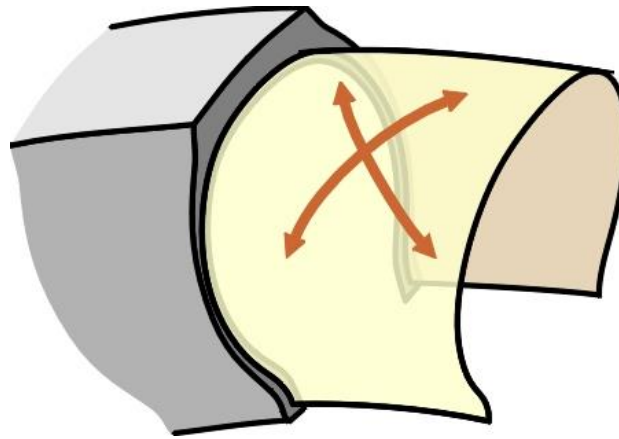


Figure 2.3 : Cross-ply tyres [4]

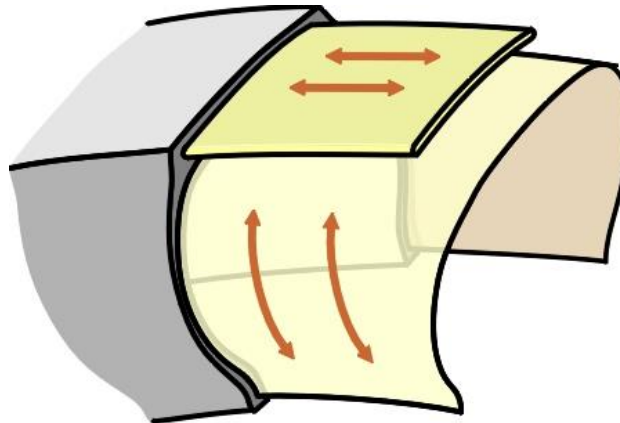


Figure 2.4: Radial tyres [4]

Cross ply (or Bias ply) is the older type of construction, where the sidewall and the tread region are made of similar construction as shown in figure 2.3. Radial tyre is advancement in tyre technology, effectively separating how the sidewall and tread region of the tyre behaves as shown in figure 2.4.

The main structural elements of a tyre are the casing assembly and the tread and belt assembly. The casing contains the volume of air and cushions the tyre. The tread and belt assembly provides the actual road surface contact responsible for minimal rolling resistance, optimal handling and a long service life.

Every modern passenger car tyre has a very complex structure and constitutes the following.

- Tread
  - Tread – High mileage/road grip/water expulsion
  - Joint-less cap plies – enable high speeds
  - The steel - cord belt plies – optimise directional stability and rolling resistance
- Casing
  - Textile cord ply – maintains inflation pressure and tyre's shape
  - Inner liner – makes the tyre airtight
  - Side wall – protects from external damage
  - Bead core – ensures firm seating on the rim
  -

Tread is the outmost surface of the tire that comes in contact with the road surface as shown in figure 2.5. Its function is to provide a good amount of traction, while being durable. Tread also contains patterns of grooves, lugs, voids and sipes. The function

of the tread pattern is to expel any water that may come between the road surface and the tyre in order to maintain good contact with the road surface.

Bead part of the tyre as shown in figure 2.5, comes in contact with the rim of the wheel. The bead needs to tightly sit on the rim as to hold to the air in the tubeless tyre, it should not let the tyre rotate circumferentially as the wheel rotates. It is the main interface that transfers the normal load from the contact patch to the rim. Hence it should be able to support the load.

The sidewall is the part between the tread and the bead as shown in figure 2.5. It consists of mainly of rubber reinforced with fabric or the steel cords that make the ply.

Plies are the strong fabric or steel cords embedded in the rubber to hold the shape of the tyre when the tyre is inflated. These plies play a significant role in the load carrying capacity of the tyre and the inflation pressure possible.

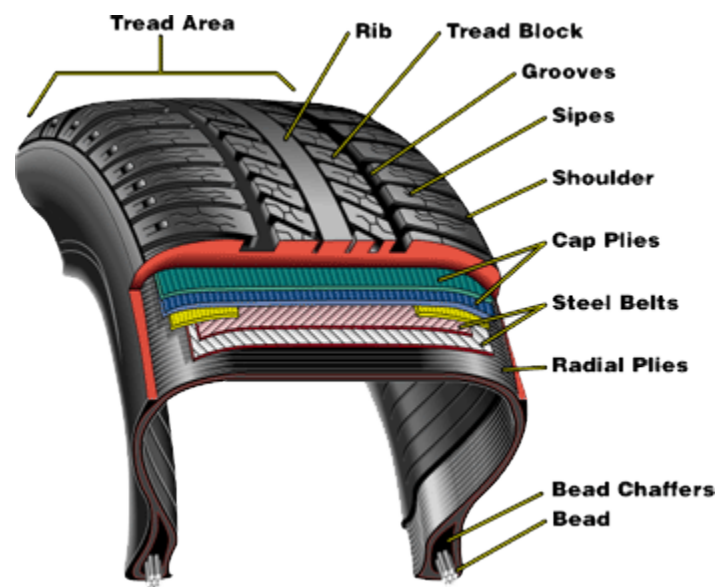


Figure 2.5: Structure of a tyre [5]

### 2.1.2 Mechanism of load carrying

The mechanism of load carrying in tyre is quite interesting. The air doesn't carry any load on its own, but the inflation pressure creates tension in the tyre wall. As the tyre is normally loaded it creates a difference in tension radii as depicted in figure 2.6. The difference in tension effectively carries the load onto the rim. So the upper part of the tyre sidewall is under maximum tension essentially lifting the rim using the bead. In an ideal case all the load is carried by this difference in tension and not directly by the sidewall part close to the contact patch [4].

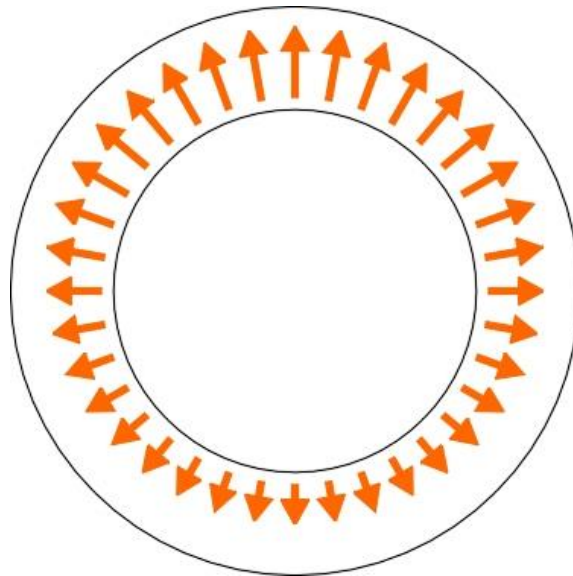


Figure 2.6 : Tension in a tyre [4]

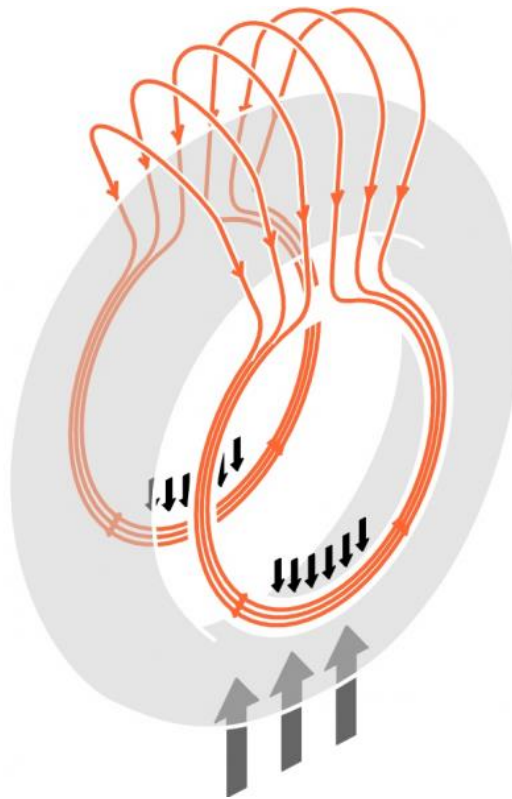
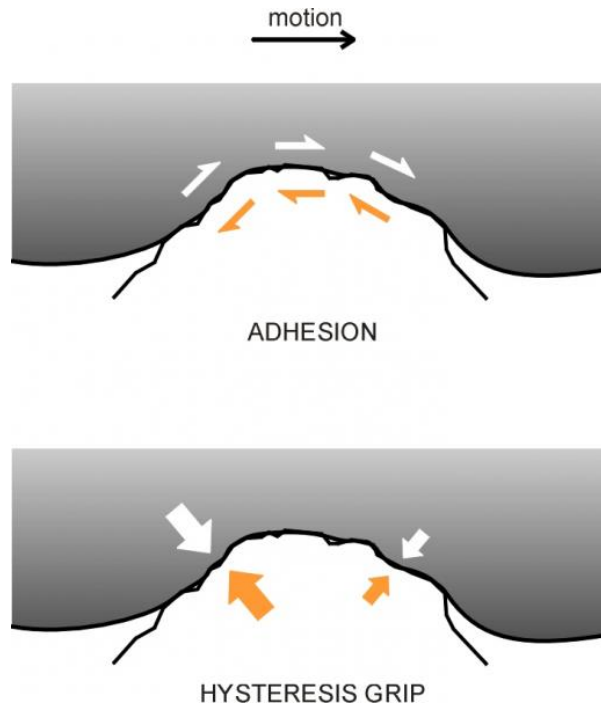


Figure 2.7: Load path in a tyre [4]

### 2.1.3 Mechanism of road grip

There are two primary effects responsible for the road grip.

- Molecular adhesion
- Hysteresis grip



**Figure 2.8:** Adhesion force and hysteresis forces are shown in the upper part and lower part of the figure respectively; the orange arrows show the force exerted on the tyre. [4]

### 2.1.3.1 Molecular adhesion

Adhesion is the force resulting from interactions at the molecular level at the tyre/road interface. It is also generally known as friction between two surfaces. This is again divided into static and kinetic friction.

The maximum frictional resistance force can be calculated by multiplying normal force  $N$  multiplied by Coefficient of friction  $\mu$  (static)

$$F = \mu * N$$

Where  $\mu$  is a fixed value dependent on the combination of the two materials in contact. The frictional force is therefore independent of the surface area.

After the object starts moving, the resistance is generally reduced to a lower value,  $F_s$ . This value of sliding friction is proportional to  $N$  as well.

$$F_s = \mu_s * N$$

There are various models that explain this phenomenon. Friction is caused by electrical forces between the molecules of both surfaces.

### 2.1.3.2 Hysteresis grip

Rubber is a material that can absorb lots of energy during loading and unloading. The path that the rubber follows during loading is different compared to unloading due to this absorption of energy, this property is called hysteresis.

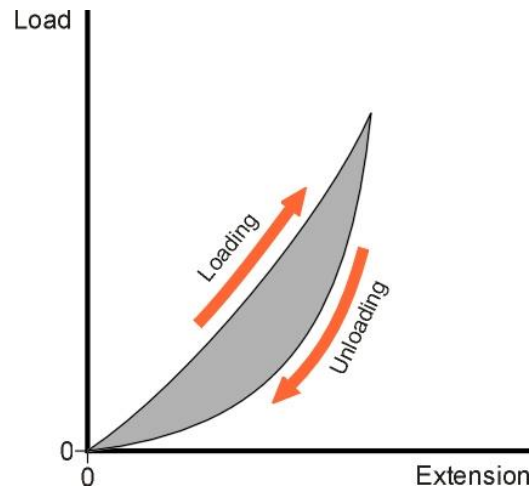


**Figure 2.9: Hysteresis curve [4]**

Compared to harder surfaces such as plastic or metal, a rubber surface can better hold on to the irregularities in the road surface. The irregular peaks on the road surfaces create indentation on the tyre surface. Now the surface created due to the indentation gives additional grip otherwise not present in two rigid surfaces.

When the vehicle is moving and there is some acceleration or deceleration, the vehicle will tend to drag the tyre tread surface along the road surface. As the material is continuously undergoing compression and expansion due to various asperities along the road, the hysteresis comes into play, which increases the forces on the compression (loading) side of the indentation compared to expansion (unloading) side. The resultant is a horizontal force. This force still does not include the shear forces created by surface friction.

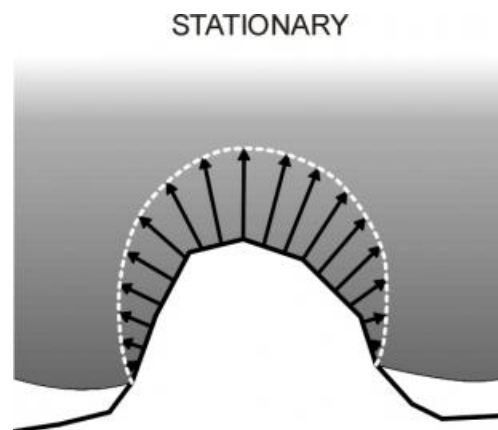


**Figure 2.10: Normal force on a road asperity when stationary [4]**

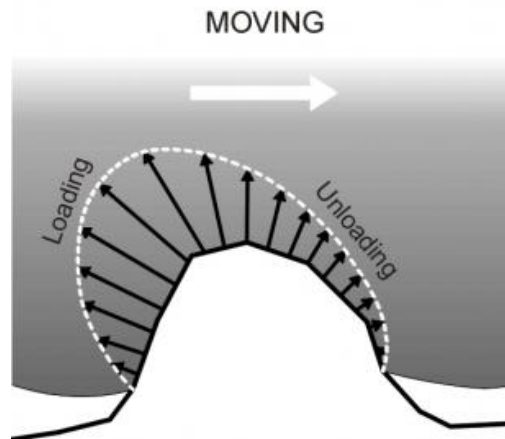


Figure 2.11: Normal force on a road asperity when moving [4]

The total horizontal force is now the sum of forces due to both adhesion and hysteresis, while force due to adhesion is directly proportional to the normal force, the adhesion force is a function of normal load and sliding speed and sliding speed direction on a micro level.

### 2.1.4 Mechanism of Rolling Resistance

Contribution to rolling resistance is accounted for by three important phenomena. They are tyre deformation in contact patch, the rotational aerodynamic drag of the wheel and slip between tyre and road or wheel rim. Tyre deformation constitutes a major part of rolling resistance and is mainly because of bending of the tyre crown at the leading and trailing edge of the contact patch and bending or bulging out of the side-wall because of the load on tyre structure, compression of the tread throughout the contact patch area and finally shearing of tread and sidewall elements. These phenomena cause a deformation induced viscoelastic energy loss in the tyre [6].

The belt part of the carcass is generally made of belt and is non elastic and of fixed length. There is rubber beneath and above this belt and in the case of bending of tread at leading and trailing edges of the contact patch it would mean that the rubber layer inside gets compressed and the rubber layer outside this belt expands. Now this change in radius at the edges and rubbing of layers will manifest itself in hysteresis loss and hence contributing to rolling resistance [7].

In case of braking or acceleration the slip factor contribution to rolling resistance becomes significant. There is a portion of the tyre where the material shall stick to the road and the rest part of contact patch shall slip against the road surface. The rotational aerodynamic drag depends on the tread design since the tyre has to overcome this to be able to keep rotating at constant velocity. The contribution of rotational aerodynamic drag becomes significant at high wheel velocities [7].

The major contributors to creation of resistance to rolling of tyre on a straight and flat road surface are energy dissipated in the process of rolling and aerodynamic drag. The energy absorbed in heat is a manifestation of hysteresis forces because of radial deformation of the tyre. The hysteresis damping tends to produce higher pressure by acting radially inward in the front part of the contact patch and the opposite happens in the rear half of the contact patch. This leads to a shift in centre of normal pressure in the contact patch area in the direction of rolling as shown in figure 2.12. The shift in pressure centre produces a moment about the tyre centre opposing the rolling. The other component of the radial force acting on the tyre structure is the shear force. This force exists between the tyre road interface which opposes the longitudinal motion or acts in negative x-direction. The moment of this shear force cancels the rolling

moment. However, for the overall force diagram of the system to be balanced so that the vehicle rolls at a constant longitudinal velocity, there has to be a force at the centre of the hub pushing the wheel longitudinally or acting in positive x-direction and must measure exactly equal to the longitudinal negative shear force at tyre and road interface [8].

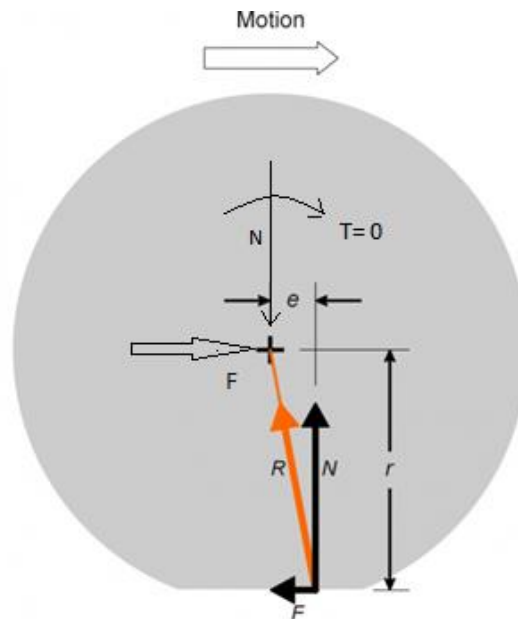


Figure 2.12: Shift in pressure centre during free rolling [4]

## 2.2 Influence of tyre parameters on rolling resistance

Various factors affect rolling resistance like tyre radius, width, inflation pressure, normal load and velocity. Over years, rolling resistance data have been obtained for various types of tyres from laboratory tests that are used for comparison of rolling losses and effect on fuel consumption. Many such models are polynomial expressions and have parameters like velocity, normal load and inflation pressure [9]. These expressions have coefficients that are determined through curve-fitting to experimental values. This approach is specific for each kind of tyre and although it predicts an accurate representation, it does not provide a physical understanding of tyre rolling resistance phenomena. Hence it is important to know how each of the parameters influence rolling resistance and how they are varied.

### 2.2.1 Influence of tyre size

Tyre sizing is a critical parameter with respect to many aspects of a vehicle other than rolling resistance losses, for example vehicle handling. It is hence indispensable from vehicle design and loss point of view in the early phase of vehicle platform development. While varying tyre size, other parameters are kept constant, for example, inflation pressure, longitudinal velocity, loading capacity and possibly tyre width. It may be important to note that for increasing the tyre outer diameter while keeping same loading capacity, it is observed that the size of rim needs to increase and simultaneously sidewall height should reduce. Increasing tyre diameter decreases vertical deformation for the same contact patch length from the pure geometry point of view, when the tyre is considered in terms of a perfect circle. Even though this might seem purely theoretical, it projects an idea that decreasing the vertical deformation shall practically mean low transition of radius on the leading and trailing edges of the contact patch and hence bending of tyre tread region is lower for a bigger diameter which results in lower hysteresis losses [6].



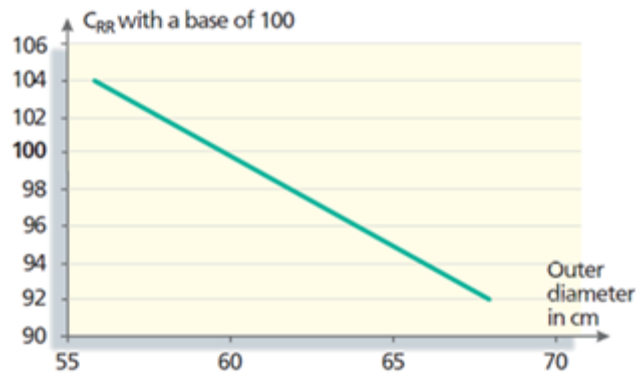


**Figure 2.13: Rolling resistance coefficient of tyre 175/70 R14 with outer diameter at 2.1 bars as per the ISO 8767 standard (with base 100) [6]**

Figure 2.13 shows a plot of rolling resistance with respect to tyre outer diameter from experimental data for a radial, passenger car tyre. A value of 100 is assigned to a tyre with outer diameter of 60 cm and the rolling resistance coefficient value corresponding to another tyre diameters are linearly scaled. The dependence linearly decreases in the range of tyre diameters shown [6].

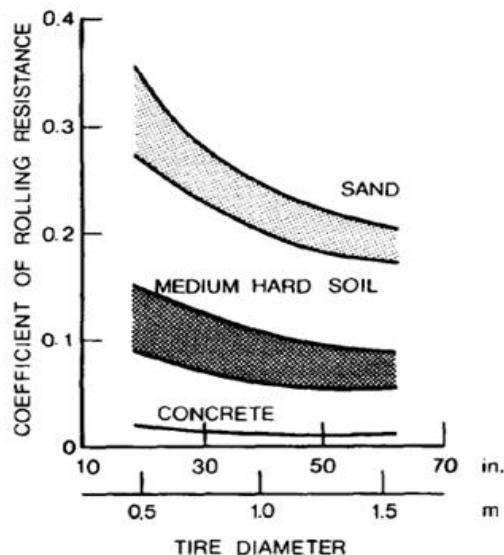


**Figure 2.14: Rolling resistance coefficient change with tyre diameter and surface types [10]**

Wong illustrates a plot from experimental data, between rolling resistance coefficient and tyre diameter in figure 2.14. On hard turf like concrete, the effect is very less pronounced, however, at medium to hard ground the reduction of the rolling resistance coefficient with an increase in tyre diameter can be observed distinctly. With deformable surfaces, the effect is magnified [10].

Figure 2.15 shows rolling resistance coefficient data at two different speeds of 20 mph and 50 mph for increasing tyre size for the radial type. The investigation suggests a marked lowering of rolling resistance coefficient with an increase in tyre size from 13 inches to 15 inches, at both speeds. The decreasing trend is in accordance with previous plots.



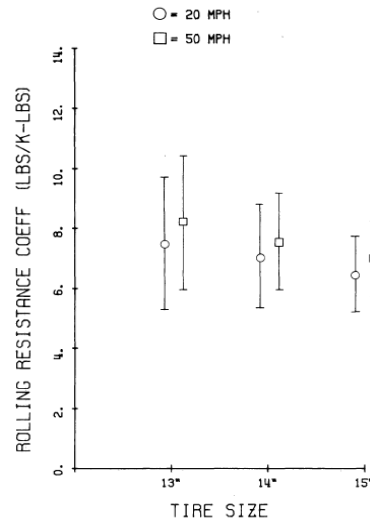


**Figure 2.15: Rolling resistance coefficient change with tyre size [11]**

For same load on a level road surface, the rolling resistance coefficient decreases for the decrease in an aspect ratio of the tyre, though not very remarkably [12]. This may be understood as saying that the more the tyre width compared to section height, the lesser is the rolling resistance coefficient. The contact patch area increases while increasing width thereby decreasing the force sustained by each element in the patch. As such, the compression of each element in the tyre is lesser compared to those of a tyre with a smaller width. Hence the hysteresis loss is lower. Hence, the energy for overcoming the loss is lower and rolling resistance decreases. However, an increase in tyre width leads to an increase in aerodynamic drag [10], which is a significant factor at high speeds when looking at rolling resistance coefficient.

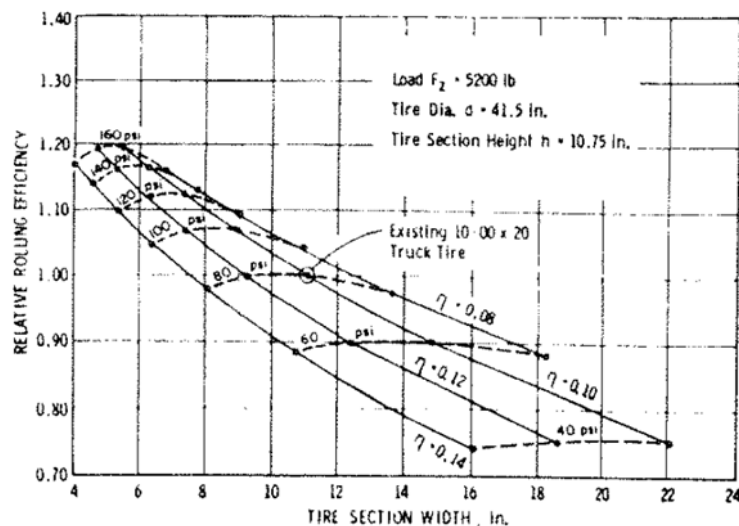


**Figure 2.16: Influence of the aspect ratio of fixed tire size and load carrying capacity [13]**

Figure 2.16 plots relative rolling resistance efficiency with respect to change in tyre width at different tyre inflation pressure levels for a truck tyre. Relative rolling resistance efficiency is defined as a ratio of normal load to rolling resistance. The tyre diameter, tyre vertical load, section height and tyre tread thickness are kept constant and at each inflation pressure a section width is plotted for the given load. The study suggests that moderate improvement in relative rolling efficiency or decrease in rolling resistance coefficient is possible by means of increasing pressure and having low tyre width [13]. However the speed at which the data is measured is not mentioned.

## 2.2.2 Influence of tyre inflation pressure

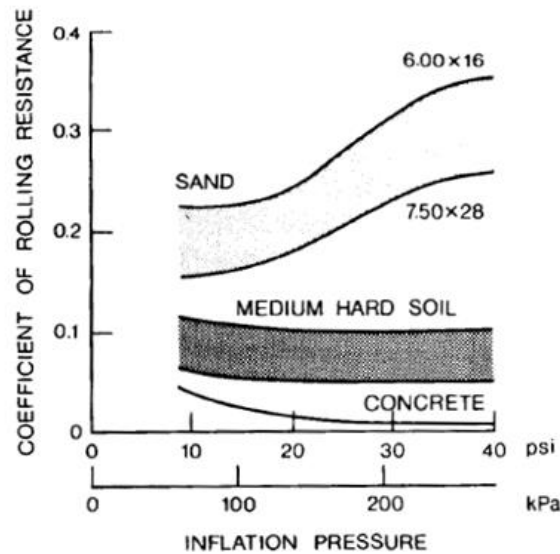


Figure 2.17: Variation of rolling resistance coefficient with inflation pressure of tyres on various surfaces [10]

Tyre rolling resistance decreases with increase in pressure on level road surface as other parameters are kept constant. As the pressure increases, the tyre holds its shape more firmly and vertical deflection decreases. Thus the deformation of rubber is lesser compared to that in a tyre with lower pressure. Hence the hysteresis losses reduce thereby decreasing rolling resistance in case of level road surface which is reflected in the figure above [10]. In case of deformable surfaces, deformation of other contact surface which is the ground is taken into consideration for overall deformation. As inflation pressure reduces, there is a lot of bending and shearing of tyre sidewall and tread region, which amounts to losses in the rubber resulting in an increase in rolling resistance [6].

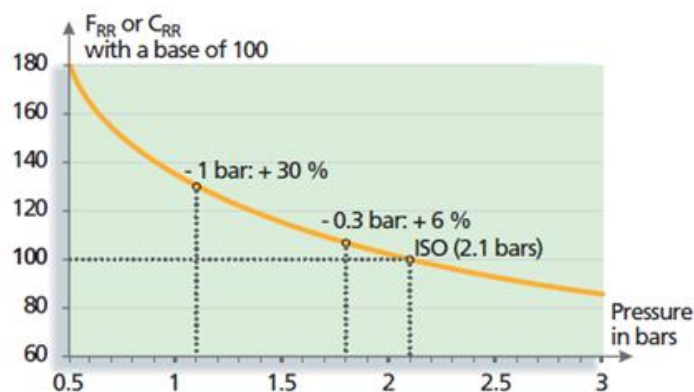
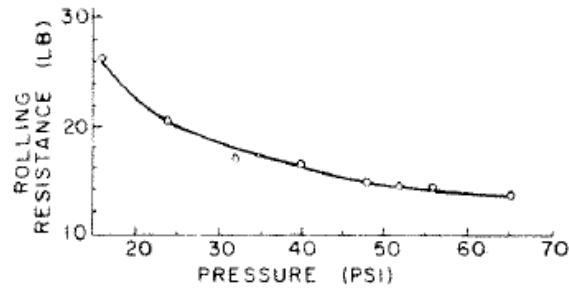


Figure 2.18: Rolling resistance measures at 2.1 bars as per the ISO 8767 standard [6]

Figure 2.18 has a value of 100 for the rolling resistance coefficient value of at 2.1 bars. The values corresponding to the rest of the pressure values are linearly scaled. The coefficient reduces as the pressure increases indicating lowered hysteresis losses at higher inflation pressure. The dependence tends to be less linear in the region of low tyre inflation pressure as can be inferred from the figure, compared to the region of nominal tyre inflation pressure.



**Figure 2.19: Dependence of rolling resistance on inflation pressure for the FR78-14 tyre tested at 1280 lbs load and 60 mph [14]**

Figure 2.19 illustrates the variation of rolling resistance with respect to tyre inflation pressure ranging from 16 to 64 psi, which is approximately 1.1 to 4.4 bars, for an old radial car tyre FR78-14. The rolling resistance data depicted in the figure is concurrent with trend obtained from pressure influence in previous references.

### 2.2.3 Influence of normal load

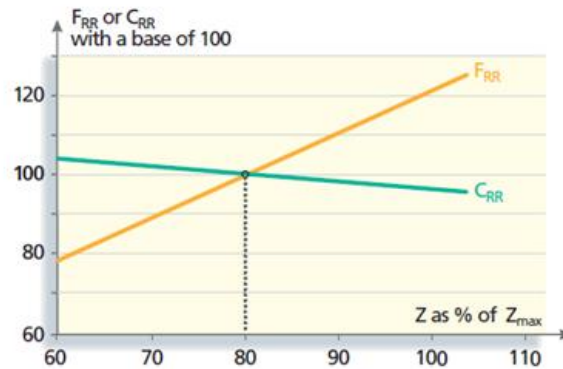


**Figure 2.20: Rolling resistance measured at 80% of the tyre's maximum load capacity as per the ISO 8767 standard [6]**

As understood from section 2.1.4, an increase in normal load will increase radial deformation of tyre elements. The rolling moment produced due to shift in pressure centre will now increase because of an increase in the vertical component of hysteresis damping, thus increasing rolling resistance force. In terms of tyre behaviour, this may be understood as more bending and shearing of the tyre structure as the normal load applied increases [6]. The same is depicted in the figure 2.20. The rolling resistance coefficient, however, is a function of the modelling of the hysteresis damping.

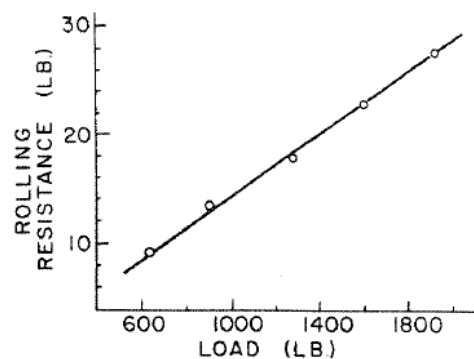


**Figure 2.21: Dependence of rolling resistance on wheel load for FR78-14 tyre tested at 32 psi pressure and 60 mph speed [14]**

Figure 2.21 shows the linear dependence of equilibrium rolling resistance (in lbs) on normal load. Rolling resistance increases as tyre load increases from 640 to 1280 lbs (290 to 580 kilos approximately) at 32 psi (2.2 bars) and 60 mph (97 km/h) for an old radial car tyre, FR78-14 [14].

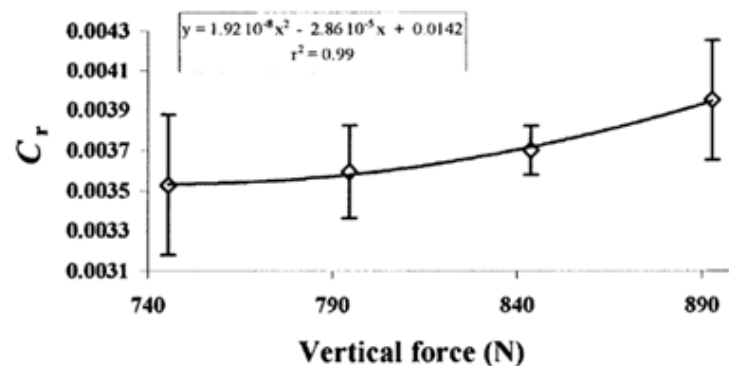


Figure 2.22: Coefficient of rolling resistance as a function of the total vertical force applied to the bicycle tyres. [15]

In a study to determine the effect of normal loading on rolling resistance for cycling performance, racing bicycle of 9.8 kg with clincher tyres were used by a cyclist and then pay-loaded with extra weight in a backpack. The coefficient of rolling resistance was determined by coasting method, indoors. The value of the coefficient was observed to increase with increase in normal loading, quite in contrast to the trend observed in passenger car tyres, figure 2.20. This is shown in figure 2.22. Hence the behaviour of RRC with vertical force is specific to a type of tyre and may increase or decrease.

## 2.2.4 Influence of longitudinal velocity

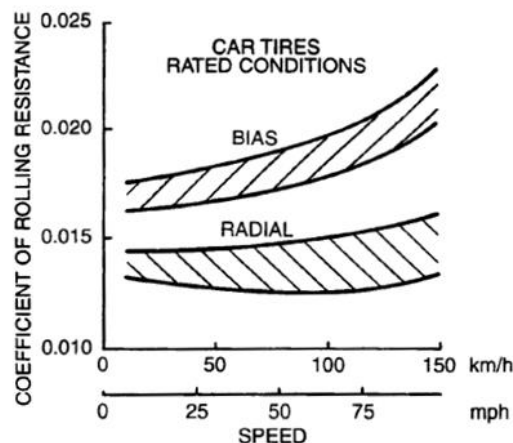
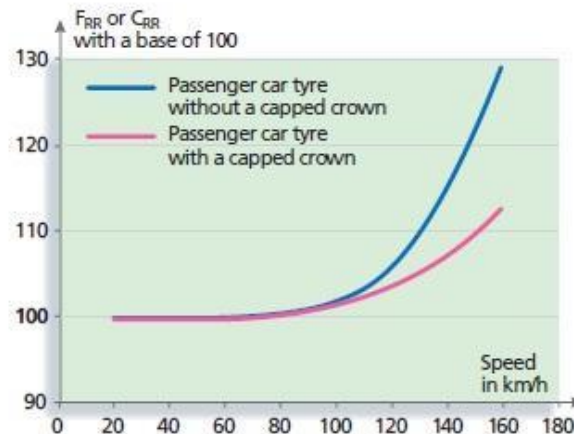


Figure 2.23: Variation of RRC of radial and bias-ply car tyres with speed on smooth and flat surface under rated load and inflation pressure [10]

Wong illustrates a plot of longitudinal velocity with respect to rolling resistance coefficient as shown in figure 2.23. For radial car tyres, it can be observed that the plot is quite flat till 100 km/h and then increases notably. A similar plot (see figure 2.24), from Michelin (with base 100 at 80 km/h and constant loading of 80% of load bearing capacity at 2.1 bar) for passenger car tyres with and without capped crown also suggests that the graph is very much constant till 100 km/h, slightly rises till 120 km/h and then shoots because of aerodynamic drag [6]. From section 2.1.4, it may be noted that the hysteresis damping which results in a shift in centre of pressure is not enough to explain or model the complete velocity dependence. At higher velocities,

the rotational aerodynamic drag must be taken into account which has been referred to in section 3.6. The relatively flat plot at velocities below 100 km/h suggests that much of the hysteresis damping is independent of velocity in this region.



**Figure 2.24: Base 100, rolling resistance measured at 80 km/h for both tyres as per the ISO 8767 standard [6]**

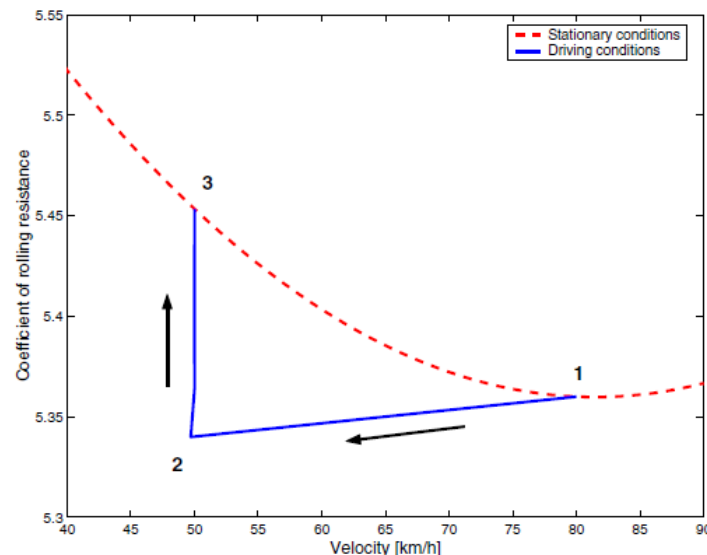


**Figure 2.25: Stationary conditions at 80 km/h followed by a longer period of 50 km/h. Y-axis is RRC multiplied 1000 times. [16]**

Tyre rolling resistance can hardly be explained purely with velocity. Change in velocity is accompanied by a change in temperature in the air inside the tyre, shoulder region soon. Hence a model was developed to include changes in temperature with slow and fast change in velocity. Stationary conditions are defined for rolling resistance for velocity by driving the vehicle on a straight road for a long time and the stationary RRC is obtained for the corresponding tyre shoulder temperature. The thermodynamic tyre behaviour was included by energy equation and principle of heat flow. It was observed that while driving, for example, at 80 km/h the dotted line in figure 2.25 represents a stationary condition. As the speed was lowered to 50 km/h in few seconds, the RRC reduced transiently according to the blue line from point 1 to point 2. This RRC value is higher than the value at a stationary temperature at 50 km/h since the tyre was still hot. After being driven at 50 km/h for a long time, the tyre temperature dropped and the RRC value jumped back onto the dotted line which is point 3 [16].

### 3 Modelling

This chapter presents the methodology and various phases of the thesis to achieve the tyre rolling resistance model. There are several phases of the model that implement improvements to different phenomena observed. At each phase results were compared to experimental data obtained from the literature.

#### 3.1 Basic Assumptions

Rolling resistance coefficient (RRC) can be defined in many ways. It is common in the vehicle industry to define rolling resistance as the ratio of rolling resistance force to normal force.

$$RRC = \frac{F_x}{F_z}$$

But for the purpose of this work, most of the calculations have assumed the other definition based on the offset “e” of the normal pressure distribution along the contact patch length. Where rolling resistance coefficient is the ratio of the offset length of the deformed radius of the tyre.

$$RRC = \frac{e}{R}$$

Some of the other assumptions made throughout the development of the tyre model for rolling resistance are as follows.

- The contact patch shape is a perfect rectangle
- Contact width is equal to section width
- Contact patch length is a function of vertical deformation purely on the basis of geometry. ( $L=f(\Delta z)$ ))

#### 3.2 Radial spring and damper distribution

The tyre contact patch is considered to be constituted of identical radial elements, each of which is a combination of a linear spring and a viscous damper. The vertical load on the tyre causes radial deflection in spring and damper elements in the contact patch, at the bottom of tyre as shown in figure 3.1. The total normal force on the tyre is then the summation of elemental spring and damper forces throughout the contact patch where the spring and damper forces are given as follows.

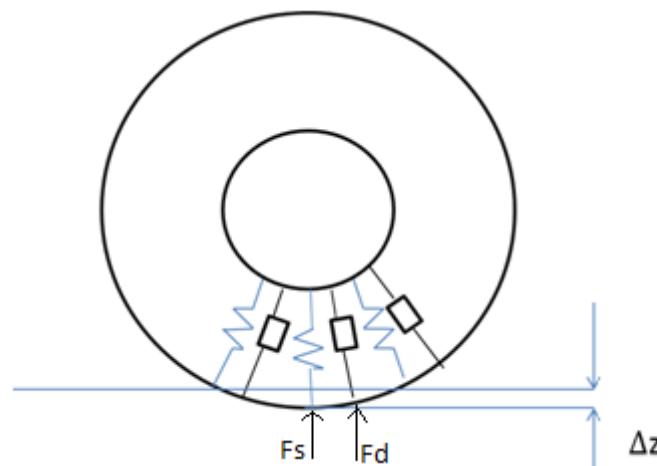


Figure 3.1 Distributed spring and damper elements in tyre

Where  $F_s$  = elemental spring force as shown in figure 3.1,  $K$  = elemental spring stiffness and  $z$  = vertical component of radial deformation of element at an angle  $\theta$  from centre line of contact patch as shown in figure 3.2.

Where  $F_d$ = elemental damper force as shown in figure 3.1,  $C$ = elemental damping coefficient and  $z_{dot\theta}$ = vertical component of radial deformation velocity of element at an angle  $\theta$  from centre line of contact patch as shown in figure 3.2.

The vertical displacement of any element in the tyre contact patch can be calculated from the equation of perfect circle as,

Where  $R$  is the unloaded radius of inflated tyre,

$\theta$ = angle between the radius through middle of contact patch and the radius through any element.

$\theta_{\max}$  = angle between the radius through middle of the contact patch and the radius through the element at the leading or trailing edge of the contact patch

The position of this element along the contact patch with axis configuration as shown in figure 3.2 can be stated as follows.

Total normal force on the tyre can be given as below.

The following plots of spring and damper forces separately with respect to the elements in contact patch can be added to obtain overall normal force.

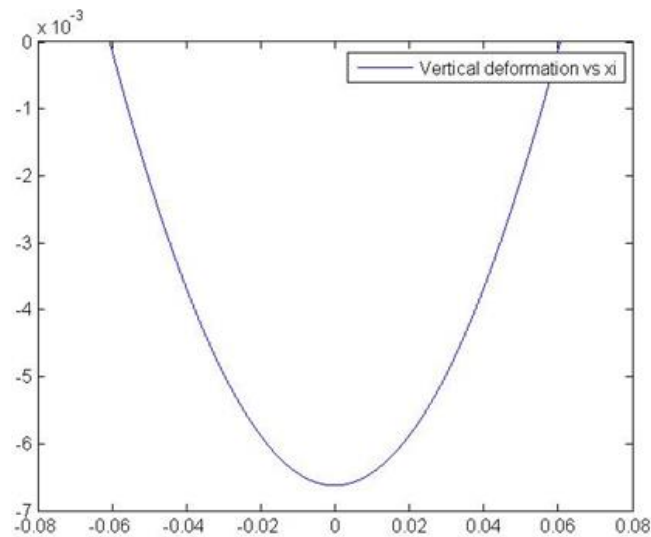


**Figure 3.3 : Vertical deformation of each element along contact patch (metres) with maximum deformation of 6.6 mm**

Note that the spring force is part of the equation of perfect circle and appears parabolic here because of scaling. This spring force is essentially symmetric about the z-axis in the figure 3.3. Adding this elemental force throughout the contact patch shall give us a total of zero force.

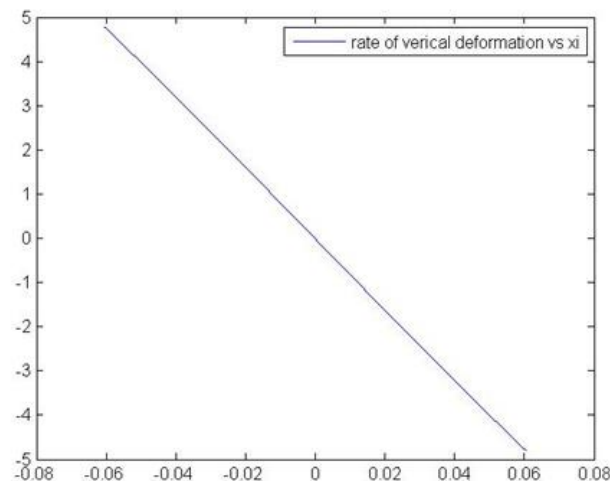


**Figure 3.4: Rate of Vertical deformation of each element in contact patch (metres)**

The above plots have been obtained for the conditions of normal load = 5 kN, tyre inflation pressure = 250 kPa, longitudinal speed = 80 km/h and number of contact patch element = 100.

The damping force can be seen with respect to rate of vertical deformation of elements throughout the contact patch in figure 3.4. This force is not symmetric about the z-axis and adding this elemental force throughout yields a resulting damper force. Because of this resulting damping force, there is a shift in the centre of pressure or the resulting normal load in the direction of rolling. This is denoted as the offset 'e'. This shift can be comprehended from figure 3.5 which shows overall normal force with respect to element position in contact patch.



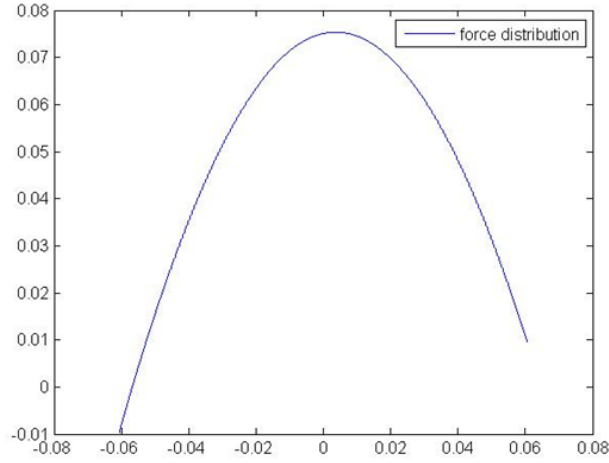


**Figure 3.5: Normal Force Distribution (165/70 R13) along contact patch (metres) at Normal load of 5 kN, tyre inflation pressure of 250 kpa, longitudinal speed of 80 km/h**

The offset calculated above can be summarized by the formula

$$e = \Sigma(F_s + F_d) * x / F_z$$

The rolling resistance coefficient is calculated as

$$RRC = e / R.$$

The spring force  $F_s$  weighed over position along contact patch gives zero value since it is a symmetric distribution across y-axis as seen in figure 3.3. Hence it is the distribution of damping force  $F_d$  that affects RRC.

The rolling resistance force is

$$F_{RR} = RRC * F_z.$$

This definition of RRC is possible to combine with a wheel which is driven or braked. An alternative definition,  $RRC = F_x / F_z$ , presumes that the torque on the wheel is zero.

Since the stiffness does not directly influence the normal load offset value, the model for damping and stiffness can be separately investigated.

### 3.3 Balloon modelling and stiffness

The vertical stiffness of a tyre is an important property of the tyre. The stiffness of the tyre comes mostly due the pneumatic stiffness of the tyre and partly due to the structural stiffness of the tyre. So in theory it is possible to have a physics-based formula to predict the vertical stiffness of a tyre using some easily obtainable parameters.

To understand the physics behind the tyre stiffness, a tyre can be considered as the balloon inflated with certain pressure. Where the tension in the balloon can be calculated using the surface tension phenomenal, where the surface tension of a bubble is dependent on the pressure difference and the radius of the bubble.

When a balloon pushes on to a flat surface the pressure at the contact region is approximately equal to the inflation pressure of the balloon. Then the area of contact is directly proportional to the normal force applied on the balloon, where the equation can be written as

$$\text{Force} = \text{Pressure} * \text{Area}$$

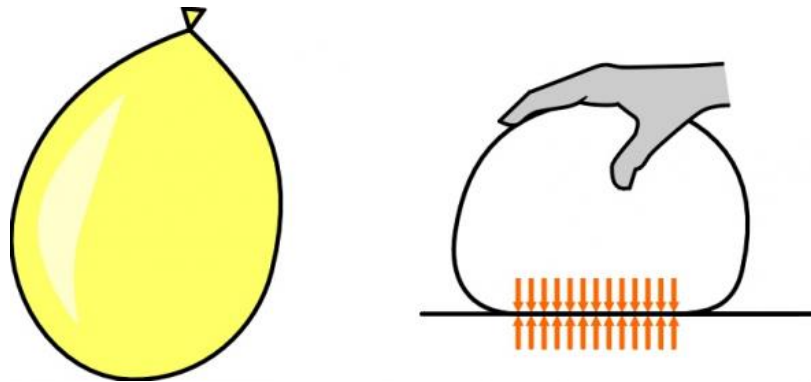


**Figure 3.6: Balloon model [4]**

So, according to this model, the material has preloaded tension due to the inflation pressure, and the load is transferred from the contact region to the hand via the balloon material, but the balloon by its own virtue does not carry any load.

But in reality the material does carry some part of the load, the proportion of this load carried due to structural stiffness is especially important at lower loads, and tends to be quite close to the stiffness predicted by the balloon at higher loads.

Figure 3.7 shows the experimental load vs stiffness relationship for radial passenger car tyres, here the slope of the curve corresponds to the stiffness of the tyre at each particular pressure. While the figure 3.8 shows the predicted load-deflection curve using the balloon model. It can be seen that, the balloon model predicts good stiffness relationship at higher deflections.

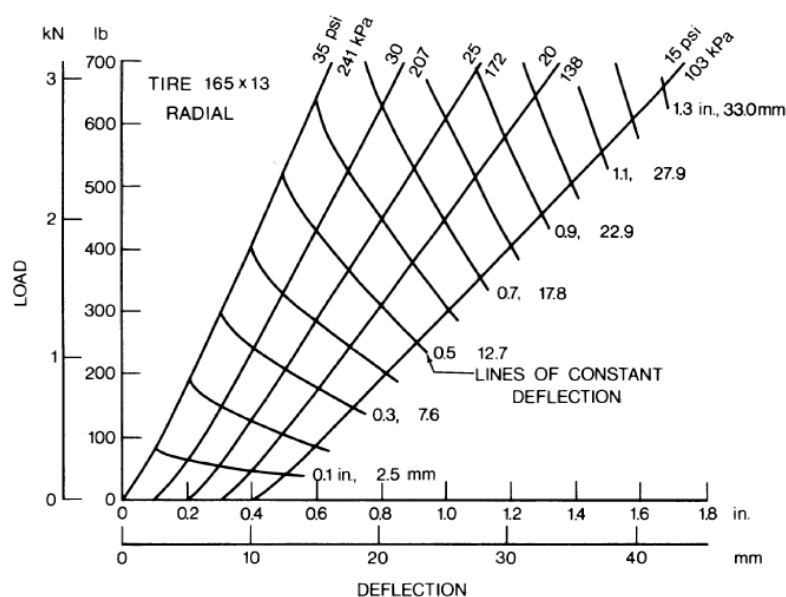


**Figure 3.7: Static load-deflection relationship of a radial-ply car tyre. [10]**

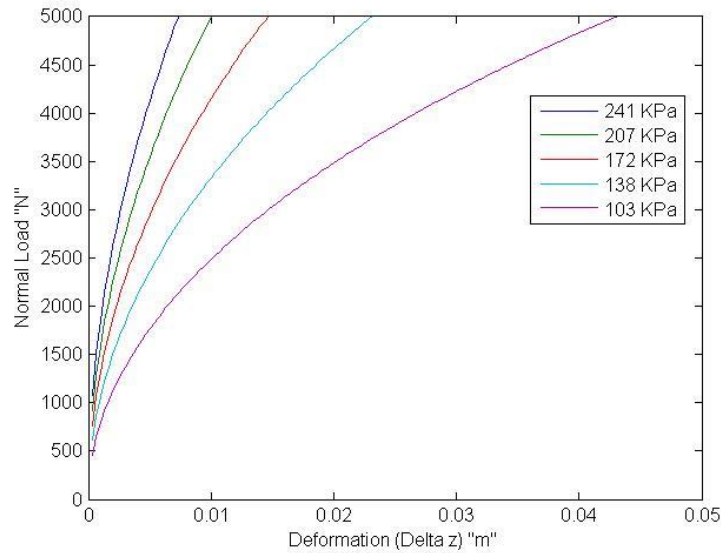


**Figure 3.8 : Load -deflection predicted from balloon model**

Unfortunately, in the working region of the tyre there is still a significant component of structural stiffness. This requires the study to investigate more accurate vertical stiffness models.

### 3.4 Constant Belt Model

Constant belt model by T. B. Rhyne [17] is a tyre vertical stiffness model based on the physics of the tyre derived from the ring model used by Koutny model without regard to thermodynamics.

The study mainly concentrates on a model based on finding the vertical stiffness of the tyre using the contained air volume in an elastic enclosure (tyre), or simply air spring applied within an inextensible ring model. Contact area has been approximated by assuming a rectangular contact patch.

The assumptions of the model are as follows

1. The tyre is assumed to be a ring of constant length at all times including loading.
2. The increased radius throughout the tyre other than transition region, away from the contact patch is called counter-deflection as shown in figure 3.9.
3. The tyre loading results in a concentric circular shape of a tyre with an increased radius which joins with the contact patch in transition with an arc of a certain radius.
4. The counter-deflection is directly dependant on the vertical deflection at the contact patch.

Variable	Definition
$R_t$	Free radius of the tire
$\lambda$	Counter-deflection = radius increase from free to loaded tire
$R_{tl}$	Radius of the tire after loading = $R_t + \lambda$
$f$	Deflection of the tire from $R_t$
$L$	Contact length
$R_b$	Transition radius from contact to $R_{tl}$
$\alpha$	Included angle of the arc of radius $R_b$

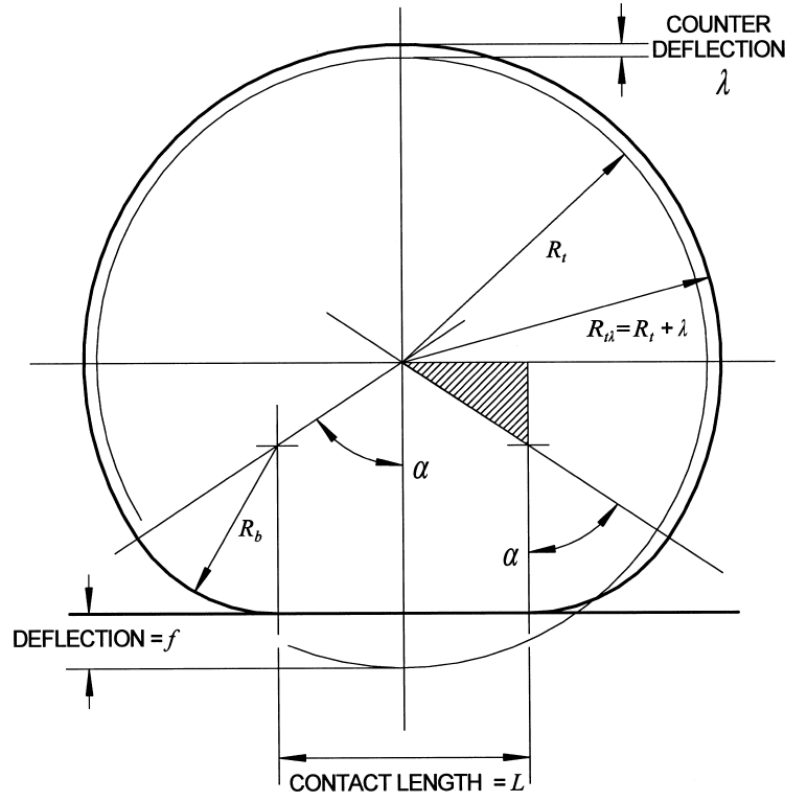


Figure 3.9: Deformation due to loading in a constant belt model [17]

The study finally gives a formula for vertical stiffness after setting the constants for counter deflection from various experimental data.

$$K_z = 0.0274 * P * \sqrt{W * D} + 3.38$$

The formula with these constants gives a good fit for a wide array of tyre data [17]. And this formula has been used in the model to calculate the stiffness of a tyre. Note that the constants take into account geometry and material property of tyre. Hence, these could be calculated separately and more accurately for a specific tyre through a set of experiments to give a better fit to the vertical stiffness equation.

### 3.5 Damping Model

The distributed viscous damper is a reasonable dependence to model the damping forces that are instrumental in causing rolling resistance so far. However the model suggests that the rolling resistance coefficient becomes zero at zero velocity which is not concurrent with experimental observation. This is evident from the section 2.2.4 in the literature review. Wong presents an experimental plot for radial tyres for passenger cars as seen in figure 2.23, which suggest that the rolling resistance coefficient versus longitudinal velocity plot is quite flat for below 50 km/h. Michelin has measurement from 2003 for passenger car tyre which depicts a flat trend for rolling resistance coefficient versus longitudinal velocity till about 80 km/h.

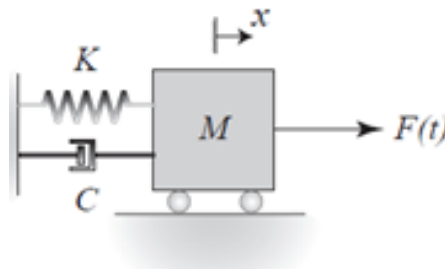


Figure 3.10: Forced spring-mass damper system

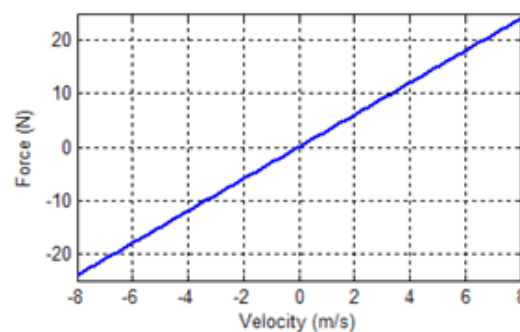


Figure 3.11: Plot for force versus velocity for mass damper system

The damper forces because of viscous damping can be depicted in figure 3.10 and figure 3.11. Damping models are not very often purely viscous for example, aerodynamic drag force is a function of the square of longitudinal velocity and not only velocity. Introduction of coulomb damping decays with time and reduces amplitude. The value is independent of frequency or velocity and can be used as a material model in this case. Here the damping model is just a constant friction model that opposes motion as shown in the figure 3.12 and figure 3.13.

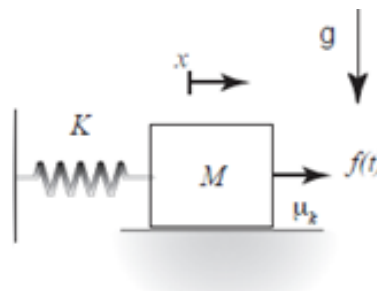
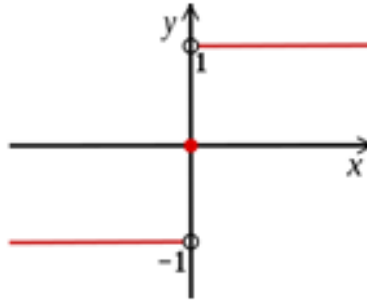
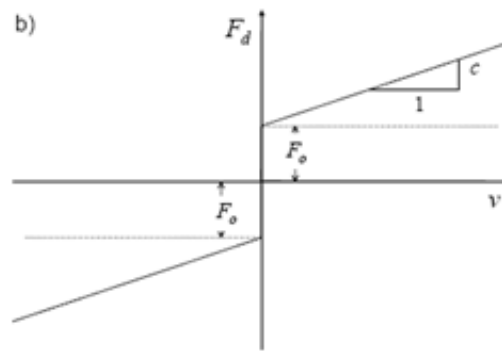


Figure 3.12: Simple coulomb friction model



**Figure 3.13: Constant friction with displacement in coulomb friction model**

The combined model accounts for damping forces even at zero or low velocities as depicted below.



**Figure 3.14: Combined force due to viscous and coulomb damping**

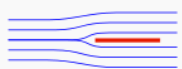
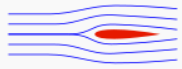
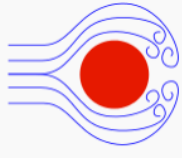
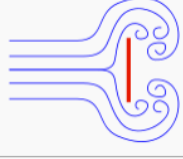
### 3.6 Rotational aerodynamic drag

While deformation in the contact patch accounts for most of the losses associated with rolling resistance, aerodynamic drag of a rotating tyre can account for as much as 15% at high speeds [6]. Rotational drag is not to be confused with the horizontal drag, which occurs when the tyre is moving horizontally. Rotational drag is the drag when the wheel just rotates without any horizontal velocity as in the case of testing on a testing machine.



**Figure 3.15: Aerodynamic drag of rotating tyre [6]**

Aerodynamic drag, also called as air resistance, is the force opposing the relative motion of the object with the air, the torque drag for which is shown in figure 3.15. The aerodynamics drag therefore depends on the relative velocity of the object with respect to air.

Shape and flow	Form Drag	Skin friction
	0%	100%
	~10%	~90%
	~90%	~10%
	100%	0%

**Figure 3.16: Types of drag and dependence on shape [18]**

There are two types of aerodynamic drag acting on any object. They are:

- **Form drag**  
Form drag or pressure drag occurs mainly due to the shape of the object. This is directly related to the cross sectional area normal to the flow of the fluid.
- **Skin friction**  
Skin friction occurs because of the friction between the fluid (air) and the skin of the object. This is directly related to the area of the surface in contact with the fluid.

All rotating objects disturb the air around them, hence there is some drag torque associated with the rotating objects. If the surface of the tyre is very flat as in the case of 'racing slick', it will mainly counter skin friction. However, if there are any grooves cut into the tread, it will have a component of the form drag as well.

The formula for the aerodynamic drag may be expressed as below.

$$F_{\text{AirDrag}} = T_{\text{AirDrag}}/R = C_d * 1/2 \rho v^2 * \text{Area}$$

Here the drag coefficient  $C_d$  is calculated from the other values in the equation. The area refers to the surface area of the tyre tread and sidewalls. This air drag is added to total longitudinal force,  $F_x$  for calculation of RRC.

The  $C_d$  depends on many factors such as the tread profile and the tread depth and so on. And there hasn't been any research done in this particular field. For this work,  $C_d$  is assumed as a constant based on the use of the same tyre shape and profile just with different dimensions.

### 3.7 Combined Model

The final model is a compilation of all the concepts explained in the preceding sections.

Tyre design parameters are

- Inflation Pressure, for a parked vehicle.
- Outer Radius
- Section Width
- Material stiffness, damping (constant in this model)
- Rim radius (no influence in this model)

Tyre operational variables

- Longitudinal velocity
- Normal load
- Temperature offset from steady state (kept at zero in this work, does not influence in this work)

All the inputs are taken in SI units to avoid conversions later.

As we know the tyre have been divided into a number of radial elements, we need to be able to calculate both displacement and radial velocity of each element. To calculate each element's radial displacement and velocity we need to first calculate maximum displacement and contact patch length.

The belt model takes  $R$ ,  $W$  and  $P$  as inputs to calculate vertical stiffness ( $K_z$ ). Using the normal load  $N$  and  $K_z$ , maximum deflection ( $\Delta z$ ) of the tyre is calculated. Using the maximum deflection and radius of the tyre, the arc angle of the contact patch is calculated.

$$K_z = f(R, W, P)$$

$$\Delta z = \frac{N}{K_z}$$

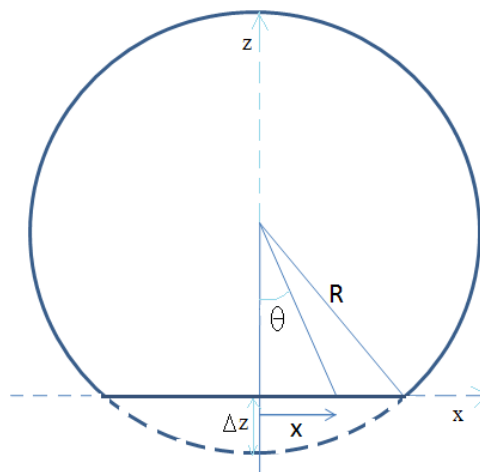


Figure 3.17: Tyre deformation from circle geometry



$$\theta_{\max} = \arccos((R - \Delta z)/R)$$

Where arc angle of the contact patch is  $2\theta_{\max}$

The position of each element is

$$x = a * \tan\theta$$

Now the vertical deformation of each element is

$$z = R * (\cos\theta - \cos\theta_{\max})$$

*Note: Vertical deformation is the vertical component of radial deformation.*

The rate of vertical deformation is

$$\dot{z} = \omega * R * \sin\theta$$

Now the vertical component of damping force each element can be calculated using the Viscous Damping coefficient coulomb/friction damping coefficient ( $C_v$  and  $C_c$ ) with  $\dot{z}$  and  $\text{sign}(\dot{z})$  respectively.

Now damping forces on each element can be integrated along the contact patch weighted with its position to get the integration of  $F_z * x * dx$  (symmetrical components are cancelled due to the weighting of the position)

This can now be used to calculate the shift in the centre of pressure “e”

$$e = \int (F_s + F_d) * x * dx / F_z$$

Where integration is over the entire length of the contact patch and  $F_z = N$ .

And the Rolling Resistance force due to damping is  $e * N$

The resistance force due to the rotational aerodynamic drag can be stated as follows.

$$F_{\text{AirDrag}} = (V_x^2) * (W * 2 * \pi * R) * C_d$$

Where  $C_d$  is the drag coefficient.

Now the rolling resistance co-efficient is

$$\text{RRC} = (e * N / R + F_{\text{AirDrag}}) / N$$

Rolling resistance force is simply given as

$$\text{“RR} = e * N / R + F_{\text{AirDrag}} \text{”}.$$

### 3.8 Final tuning coefficients and their significance

There are three model tuning parameters to tune to model to a particular type of tyre.

- Damping coefficients
  - Viscous damping  $C_v$
  - Coulomb damping  $C_c$
- Aerodynamic drag coefficient
  - $C_d$

A coulomb damping coefficient is used to tune the RRC at zero velocity in the RRC vs velocity plot. Viscous damping gives the first order curvature to the RRC vs velocity curve and the drag coefficient gives the second order curvature. Note that the coulomb damping forms a major component of the damping model for the most part of velocity dependence. The first order influence to velocity curve can hardly be seen

in the plots from section 2.2.4. The viscous damping coefficient will be much lower than coulomb damping coefficient. The aerodynamic drag part becomes significant at higher velocities and hence the drag coefficient value adjusts the curve at high velocity like 120 km/h.

There are constants (accounts for tyre material and geometry like tread thickness, sidewall height) from the constant belt model that can be tuned to a given tyre in the tyre stiffness model. Currently the constants that are given in the general formula for tyre vertical stiffness in [17] are being used.

### 3.9 Simulink Block for energy simulation

Figure 3.18 shows the Simulink block representation of the combined model developed, the block diagram also shows an example of how this model could be implemented in a simulation environment, the Matlab code uses a discrete method of integration due to the ease of implementation, the actual Matlab code can be found in the appendix.

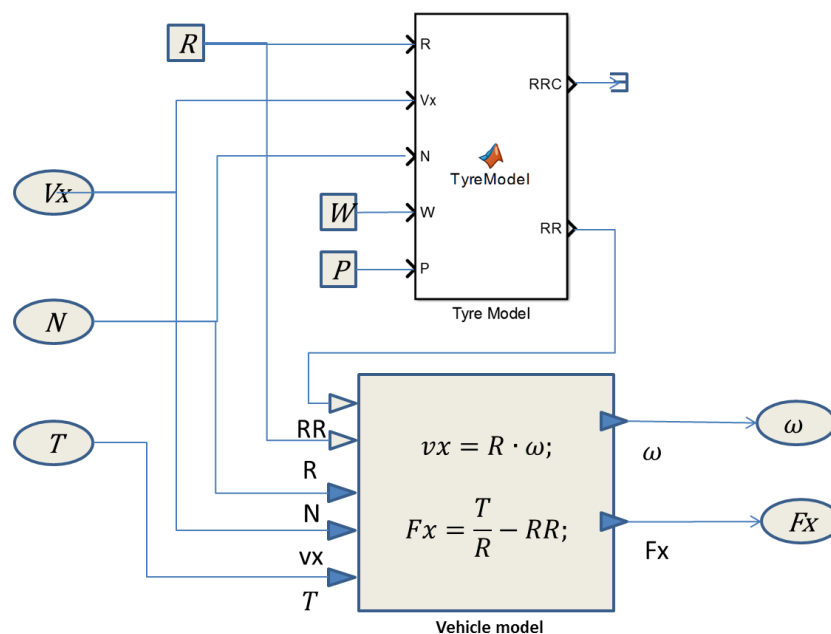


Figure 3.18: Tyre model integration in Simulink

The inputs to the model are

- Radius ( $R$ )
- Longitudinal Velocity ( $V_x$ )
- Normal Load ( $N$ )
- Section Width ( $W$ )
- Inflation Pressure ( $P$ )

The outputs from the model are

- $RRC$  = Rolling resistance coefficient
- $RR$  = Rolling resistance force.

The rolling resistance force is used outside the block as an input to LeanNova's energy simulation.

## 4 Results and Discussion

This section presents all the results obtained from the combined tyre model for rolling resistance. The results from the model in section 4.1 to 4.5 are compared to various experimental data to see how well they correlate. All the results from the model have been scaled and converted into the same units as in experimental plots to facilitate comparison between them. Section 4.6 evaluates the working of the tyre model in terms of energy consumption prediction when integrated in a vehicle model.

### 4.1 Influence of longitudinal velocity

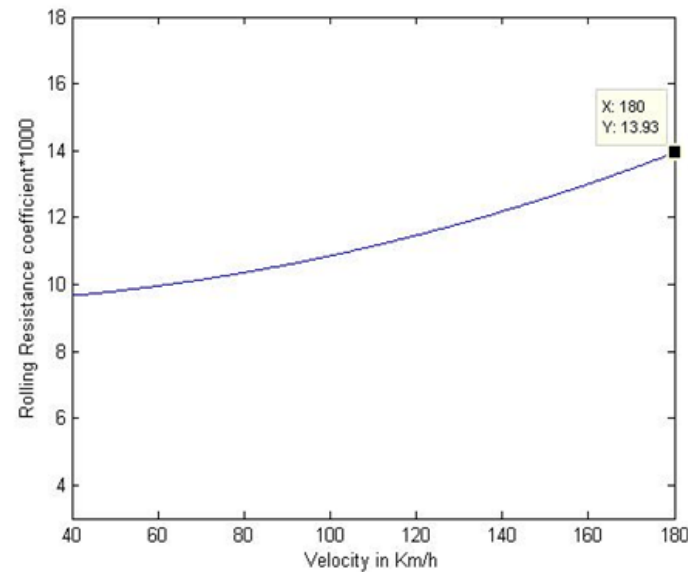


Figure 4.1 RRC vs Velocity from combined model

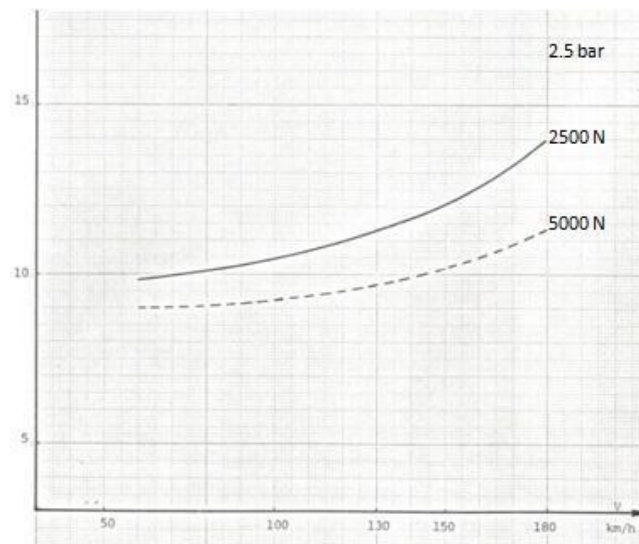


Figure 4.2 RRC vs velocity, experimental data from LeanNova (Figure 7.4, Appendix I)

Figure 4.1 shows plot between rolling resistance coefficient and longitudinal velocity, from the combined model. The x-axis represents velocity from 40 to 180 km/h, the y-axis represents 1000 times the coefficient of rolling resistance. The plot was generated for the tyre size 185/65 R15 at 2.5 bar tyre inflation pressure and a vertical load of 2500N. Figure 4. 2 show a similar plot for the same tyre and testing condition from experimentally generated data from LeanNova (Appendix I). The viscous damping

and coulomb damping coefficients were tuned so that figure 4.1 can be calibrated to data in figure 4.2. For example, at 60 km/h, the y-axis has a value of around 9.8, for 100 km/h the value is 10.5 and at 120 km/h the value is 11. At very high speed of 180 km/h, the y-axis has a value of 13.83 and the slope increases more rapidly than at lower speeds. At higher speeds the square function of velocity from the rotational aerodynamic drag component contributes significantly to rolling resistance coefficient. It is important to consider same tyre and test conditions to obtain the constants, which change for different tyre size. However, the plot obtained is generic for a tyre of given size. Different tyres in the same size category, such as summer and winter tyres, regular and off-road tyres are not accounted for. Note that the experimental data in figure 4.2 from LeanNova is old data and does not represent current generation passenger cars. Hence the actual plot can actually be slightly lower for vehicles today.

## 4.2 Influence of tyre outer diameter

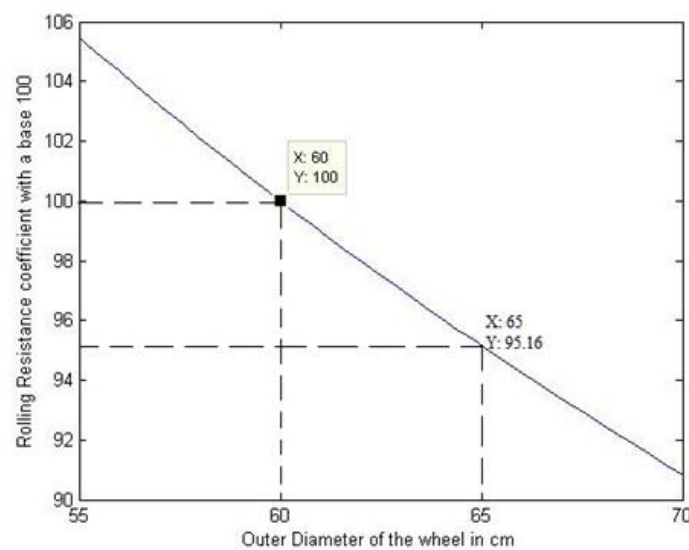


Figure 4.3 RRC vs outer diameter from combined model

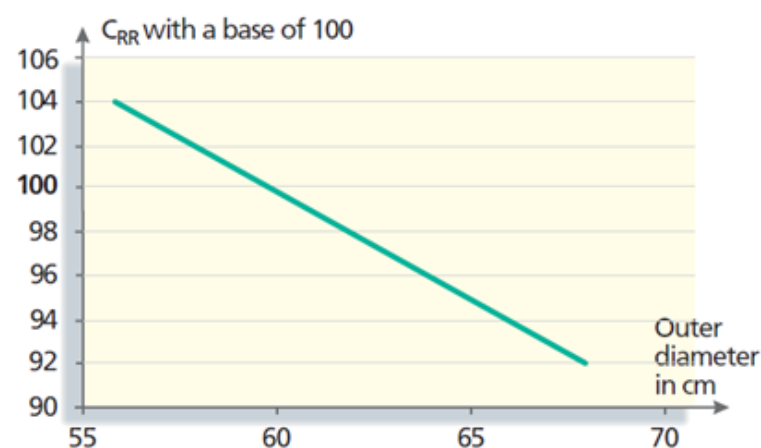


Figure 4.4 Base 100, RRC of a 175/70 R14 tyre measured as per the ISO 8767 standard [6]

Figure 4.3 shows plots between rolling resistance coefficient and tyre outer diameter, from the combined model. The x-axis represents outer radius from 55 to 70 cm. Y-axis represents coefficient of rolling resistance with a base 100, which means that the value of rolling resistance coefficient at 60 cm outer diameter is assigned a value 100 and the corresponding values for other outer diameters are linearly scaled. The plot

was generated for the tyre size 175/70 R14 with 2.1 bar tyre inflation pressure, 80% of vertical load maximum loading capacity and at 80 km/h. A plot with the actual values of rolling resistance coefficient with outer diameter is provided in Appendix I.

Figure 4.3 depicts an almost linearly decreasing trend in the range of diameter. As the radius increases, the transition at leading and trailing edges of contact patch reduces. It can thus be said that the radial deformation of elements in contact patch and the rate of radial deformation decrease. Hence the trend is quite expected. Increasing the diameter by 8.33%, from 60 cm to 65 cm, reduces the rolling resistance coefficient by approximately 4.84%.

Figure 4.4 shows a plot between rolling resistance coefficient and tyre outer diameter of the same tyre and testing conditions, from experimental data by Michelin [6]. Increasing the diameter by 8.33%, from 60 cm to 65 cm decreases the rolling resistance coefficient by approximately 5%. The combined model is seen to be in close agreement with experimental values and thus provides a very reasonable understanding of influence of outer diameter on rolling resistance coefficient. The effect of the influence of outer diameter is further tabled in a sensitivity analysis in section 4.6.

### 4.3 Influence of contact patch width

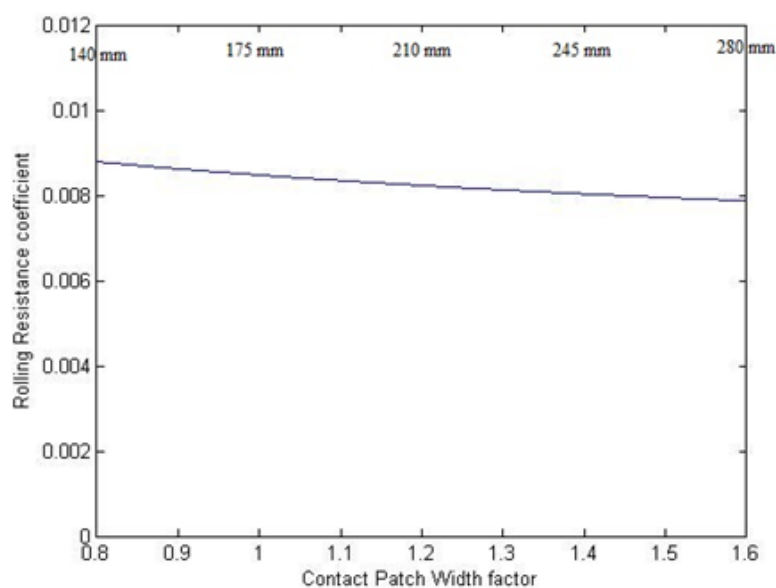


Figure 4.5 RRC vs contact patch width factor from combined model

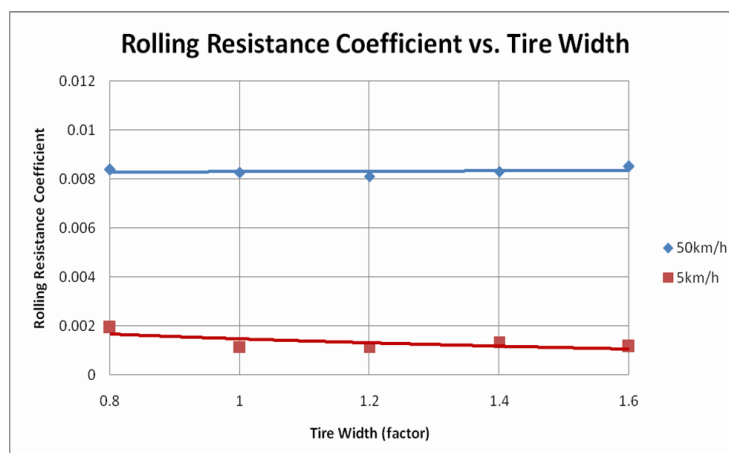


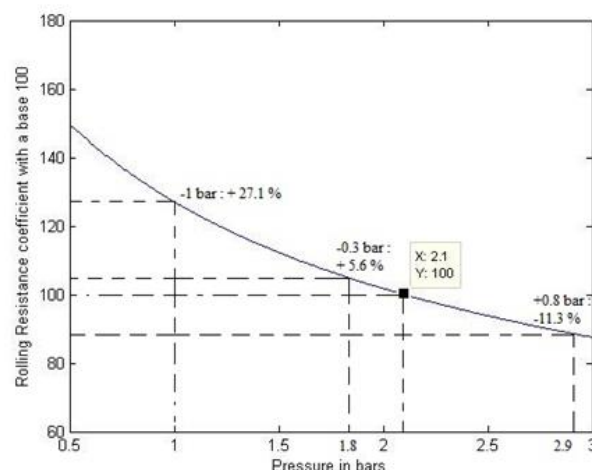
Figure 4.6 RRC versus tyre width at 50 and 5 km/h [19]

Figure 4.5 shows plot between rolling resistance coefficient and contact patch width, from the combined model. The x-axis represents the contact patch width factor where a factor of 1 is equal to 175 mm, the y-axis represents the rolling resistance coefficient. The plot was generated for the tyre size 175/70 R14 with 2.1 bar tyre inflation pressure, 80% of vertical load maximum loading capacity and at 50 km/h.

For the whole range in change of contact patch width which is a 50 % decrease, the combined model gives 10.44% increase in rolling resistance coefficient. Increase in width for the same loading, increases the elements per unit length of the contact patch, thereby reducing compression of each tread element. However, compared to the diameter influence, the effect of width appears less pronounced. From section 3.8, it may be recalled that the calculation of coulomb damping coefficient, which is the overweighing damping component, involves contact patch length. However contact patch width is involved in calculation of only the viscous damping component, which constitutes a small part of the damping model. The rotational aerodynamic drag is very insignificant at the test speed.

Figure 4.6 shows a similar plot from a finite element analysis for a truck tyre [19]. At 5 km/h, the dependence is linear and moderately decreasing and at 50 km/h the plot appears quite flat, indicating a negligible influence of tyre contact width on rolling resistance coefficient. Experimental data for exact comparison of rolling resistance coefficient values with respect to the contact patch width has not been available so far through literature review. The current comparison, although not reasonable, projects the idea that the influence of contact patch width is much lesser compared to outer diameter. The effect of the influence of tyre width is further tabled in a sensitivity analysis in section 4.6.

## 4.4 Influence of tyre inflation pressure



**Figure 4.7 RRC vs tyre inflation pressure from combined model**

Figure 4.7 shows plot between rolling resistance coefficient and tyre inflation pressure, from the combined model. The x-axis represents tyre inflation pressure from 0.5 to 3 bars. The y-axis represents the coefficient of rolling resistance with a base 100, which means that the value of rolling resistance coefficient at 2.1 bars is assigned a value 100 and the corresponding values for other inflation pressures are linearly scaled. The plot was generated for the tyre size 175/70 R14 at 80% of vertical load maximum loading capacity and 80 km/h. A plot with the actual values of rolling resistance coefficient with inflation pressure is provided in Appendix I.

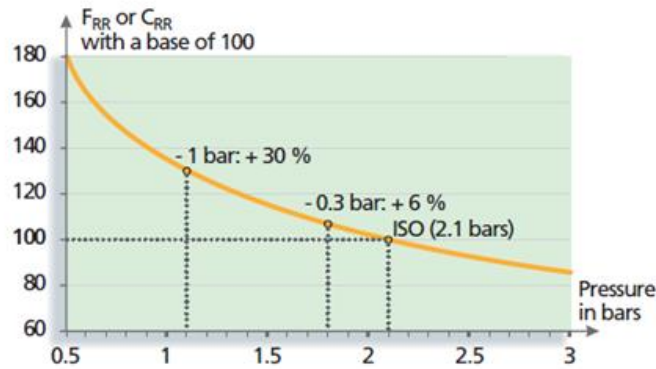


**Figure 4.8: Base 100, rolling resistance measured at 2.1 bars as per the ISO 8767 standard [6]**

Figure 4.7 depicts an almost curvilinear decreasing trend, more so at lower inflation pressure. Decreasing the pressure by 14.3%, from 2.1 bars to 1.8 bars, increases the rolling resistance coefficient by approximately 5.6%. Increasing the pressure by 38 %, from 2.1 bars to 2.9 bars, decreased the rolling resistance coefficient by 11.3 %. As inflation pressure decreases, the radial deformation of tyre treads from combined model increases and so does the rate of radial deformation. Hence the hysteresis damping increases, causing an increase in rolling resistance coefficient. With an increase in pressure, the radial deformation is low which can be translated to lesser tyre sidewall and tread bending and shearing as observed in section 2.2.2.

Figure 4.8 shows a plot between rolling resistance coefficient and tyre inflation pressure for the same tyre and testing conditions, from experimental data by Michelin. Decreasing the pressure by 14.3%, from 2.1 bars to 1.8 bars decreases the rolling resistance coefficient by approximately 6%. Note that at a very low inflation pressure, for example, below 1 bar, the difference in experimental and predicted value of rolling resistance coefficient begins to appear. This may be attributed to simple modelling of tyre rolling resistance phenomena by lumped damping model, which does not take complete material behaviour into account. The combined model is observed to be in close agreement with experimental values from Michelin in an operating pressure range of passenger car tyres. Therefore, it provides a very reasonable understanding of the influence of tyre inflation pressure on rolling resistance coefficient. The effect of the influence of inflation pressure is further tabled in a sensitivity analysis in section 4.6.

## 4.5 Influence of normal load

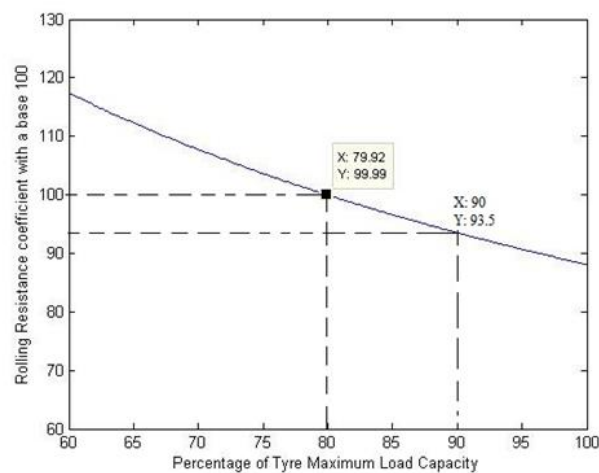


**Figure 4.9 RRC vs percentage of tyre maximum load capacity, from combined model**



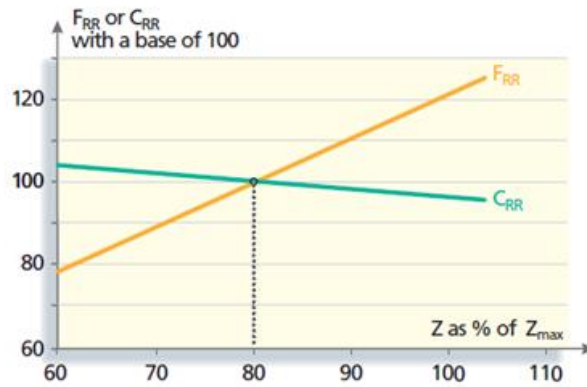


**Figure 4.10 Base 100, rolling resistance at tyre's maximum load capacity as per the ISO 8767 standard [6]**

Figure 4.9 shows plot between rolling resistance coefficient and normal load, from the combined model. The x-axis represents the tyre loading as a percentage of maximum loading capacity at 2.1 bars. The y-axis represents the coefficient of rolling resistance with a base 100, which means that the value of the rolling resistance coefficient of 80% of maximum tyre loading capacity is assigned a value 100 and the corresponding values for other inflation pressures are linearly scaled. The plot was generated for the tyre size 175/70 R14 at 2.1 bar and 80 km/h. A plot with the actual values of rolling resistance coefficient with normal load is provided in Appendix I.

The combined model suggests that tyre rolling resistance coefficient decreases with increase in normal load. Increasing the normal load by 12.5%, from 80% to 90% of maximum loading capacity, increases the rolling resistance coefficient by 6.5%. Unlike the influence of inflation pressure and tyre outer diameter, the trend obtained here is not intuitive. From the damping model, it can be inferred that the ratio of rate of vertical deformation to normal loading from the viscous damping part purely decides the behaviour. As the normal load increases, the vertical displacement increases and this ratio decrease. The rolling resistance coefficient by its definition in section 3.7 can be thought of as the sum of a constant coulomb damping and the ratio aforementioned. The overall value decreases as normal loading increases.

Figure 4.10 shows a plot between rolling resistance coefficient and tyre normal loading for the same tyre and testing conditions, from experimental data by Michelin. Increasing the normal load by 12.5%, from 80% to 90% of maximum loading capacity, increases the rolling resistance coefficient by approximately 3%. The combined model clearly overestimates the trend when compared to the experimental values. Increasing the normal load can increase temperature, which affects the damping coefficients [6]. Furthermore, the coulomb model which accounts for a major part of hysteresis damping does not take the contribution of width and material behaviour into account.

## 4.6 Energy simulation results

Energy simulations are done with respect to current nominal values of the tyre parameters and then to find out how much does each parameter vary from this value. First, power consumption due to rolling resistance at 80 km/h is found at each parameter change. Using LeanNova's energy simulation tool, identical tests are conducted while only changing the tyres for an electric vehicle. Then the Average Energy Consumption (AEC) is found in an NEDC cycle, and the sensitivity of each parameter is analysed in a full energy model of an EV.



Nominal values of tyre parameters for the current generation of passenger cars are given in the table 1. The table given the dimensions of the tyre and RRC was obtained after the model was tuned using the RRC vs Velocity curve. The power consumed due to rolling resistance alone when a car drives at 80 km/h is also shown in the table. Finally the AEC is also mentioned to see its influence in full car for comparison.

**Table 1 Nominal value of tyre parameters for current generation of passenger cars**

Outer Radius	0.305 m
Section Width	0.195 m
Inflation Pressure	2.1 bars
RRC	.0085
RR Power consumption at 80 km/h	758 watts
AEC [kWh/10km]	1.645239
ICE [litre/100km]	6.24

Table 2 shows the power consumed due to tyres only (rolling resistance power), at 80 km/h for two different outer radiuses of the tyres and the difference between these values in percentage. When power consumption by itself was observed, the reduction of 10% RRC achieved for 18 % change in outer radius.

The radius influence of the AEC in NEDC cycle for an electric car was yet to be established with certainty from energy simulation. However, from LeanNova's energy simulation, it is calculated that rolling resistance constitutes about 29% of total losses in an electric vehicle. Hence the reduction in average energy consumption for change in radii is 2.9 %, which is obtained by multiplying the percentage change in RRC to rolling resistance contribution percentage to total losses.

**Table 2 Rolling resistance power at 80 km/h for two different outer radii.**

	Low Radius	High Radius	Difference (in %)
Radius (meters)	0.28	0.33	17.86
RR Power at 80 km/h (W)	800	720	-10
ICE [litre/100km]	6.32	6.29	-0.48

Table 3 shows the power consumed due to tyres only, at 80 km/h, for two different outer section widths of the tyres and the difference between these values in percentages. When power consumption by itself was observed, the reduction is 4.4% RRC is achieved for 51.6 % change in section width. But when looking into its influence of the AEC in NEDC cycle for an electric car which is 1.4%, the parameter width seems to be able to make significant influence on the vehicle's fuel efficiency.

**Table 3 Rolling resistance power at 80 km/h for two different outer section widths**

	Low Width	High Width	Difference (in %)
Width (meters)	0.155	0.235	51.6
RR Power at 80 km/h (W)	790	755	-4.4
AEC [kWh/10km]	1.65873	1.63526	-1.4

Table 4 shows the power consumed due to tyres only, at 80 km/h, for two different inflation pressures of the tyres and the difference between these values in percentages. When power consumption by itself was observed, the reduction in 15.6% RRC is achieved for 66.7% change in inflation pressure. And when looking into its influence of the AEC in NEDC cycle for an electric car which is -4.6%, the parameter has a huge impact on the vehicle's fuel efficiency.

**Table 4 Rolling resistance power at 80 km/h for two different inflation pressures**

	Low Pressure	High Pressure	Difference (in %)
Pressure (bar)	1.8	3	66.7
RR Power at 80 km/h (W)	770	650	-15.6
AEC [kWh/10km]	1.67	1.59	-4.6

Table 5 shows the power consumed due to tyres only, at 80 km/h, for the combination of all the parameters that contribute to the nominal and low RRC values. The two modes are defined as follows.

Nominal Mode:

Tyre inflation pressure = 2.1 bar, Tyre outer radius = 0.305 m, Tyre width = 0.195 m

Low RRC mode:

Tyre inflation pressure = 3.0 bar, Tyre outer radius = 0.330 m, Tyre width = 0.235 m

When power consumption by itself was observed, the reduction is 18.2% RRC from the nominal tyre parameters in use now. But if a car currently runs on a tyre which has

the combination of parameters that contribute high RRC the power consumption can be reduced by a very significant 27%. The reduction in AEC in NEDC run for an electric car is 3.8% for nominal to low RRC mode. The reduction in average fuel consumption in the NEDC run for a conventional vehicle is 1.3% for nominal to low RRC mode. Thus, it may be observed that reduction in rolling resistance alone can make a significant contribution to fuel saving, more so in an electric vehicle. This may allude to the fact that electric vehicles do not lose so much energy in friction brakes because of regeneration. For an average reduction in rolling resistance by 30%, while keeping the vehicle design constant, the fuel consumption is reduced by about 3% to 6% and may vary depending on the type of driving cycle and vehicle [6]. This means that for a reduction of 18.2 % in rolling resistance the reduction in fuel consumption can be 1.8% to 3.6% according to Michelin [6]. The model, however, predicts the fuel consumption reduction to be 1.3%, which is on the lower side of this experimental data spectrum. This may indicate that there are other parameters that can affect tyre rolling resistance phenomena. Note that the model considers free rolling and does not include torque or the contribution of longitudinal slip to rolling resistance and the influence of transient temperature changes in different parts of the tyre. Also the experimental data taken to tune the combined model damping coefficients are old values and not entirely representative of data for present generation passenger cars.

To have an understanding of the influence of the tyre parameters on rolling resistance in electric vehicle platform, a comparison is made between the two tyres with similar load capacities which may be used on a generic electric vehicle.

tyre1: 155/70 R19 at 2.5 bars

tyre2: 175/65 R15 at 2.3 bars

The rolling resistance power calculated for tyre1 and tyre2 from combined model are 670 W and 744 W respectively. The reduction in rolling resistance is approximately 10 % from tyre2 to tyre1. From LeanNova's energy simulation, it is calculated that rolling resistance constitutes about 29% of total losses in an electric vehicle. Hence the reduction in average energy consumption from tyre2 to tyre1 is 2.9%, which is obtained by multiplying the percentage change in rolling resistance to rolling resistance contribution to total loss.

From LeanNova's energy simulation package, it is calculated that rolling resistance constitutes about 29% of total losses in an electric vehicle. The change in tyre inflation pressure from 2 bars to 3 bars was calculated to be 3.7%. A study conducted on the influence of tyre inflation pressure on fuel consumption [20] suggests that rolling resistance constitutes 27% of total losses in a conventional vehicle in NEDC run. Furthermore, the study observes that a change in tyre inflation pressure from 2 bars to 3 bars leads to a reduction in average fuel consumption by 5.2%. It can only be fair to compare two simulations that have a similar percentage contribution of rolling resistance to total vehicle losses. Hence the electric vehicle operation from LeanNova's energy simulation and the conventional vehicle simulation from the study can allow for a comparison of average consumption (fuel and energy). The study [20], suggests a slightly higher sensitivity of inflation pressure compared to the energy simulation from this thesis.

**Table 5 Rolling resistance power at 80 km/h for the combination of all the parameters that contribute to the nominal and low RRC values.**

	Nominal mode	Low RRC mode	Difference from nominal to low RRC mode (in %)
RRC*1000	8.5	6.9	-18.2
RR Power at 80 km/h [W]	758	620	-18.2
AEC [kWh/10km]	1.64	1.58	-3.78
ICE [Litre/100km]	6.24	6.16	-1.30

In summary, tyre inflation pressure is observed to be the most influencing parameter in terms of absolute contribution to rolling resistance in the considered range of parameter variation from table 2, 3 & 4. However, tyre outer radius is the most sensitive parameter with respect to rolling resistance from table 6, followed by inflation pressure and finally tyre section width. Even though outer radius seems to be the most sensitive parameter with respect RRC, its influence on the AEC values needs to be established from energy simulation (after considering final drive ratio change).

**Table 6 Parameter sensitivity to rolling resistance**

Parameter	% RR power change/ % Parameter change
Diameter/Radius	-0.56
Width	-0.086
Pressure	-0.23
Normal load	0.073

## 5 Conclusion and Future Work

In this section, a short summary of the important findings of the thesis work is presented. Some suggestions for future work are also included.

### 5.1 Conclusion

This work presents the influence of parameters like tyre size, inflation pressure, longitudinal velocity and normal load on tyre rolling resistance coefficient. It also presents each of their contributions to average fuel or energy consumption through energy simulation tool by LeanNova. The rolling resistance models were implemented in Matlab/Simulink. The important findings from the combined model and the energy simulations are briefly discussed in the sections below.

#### 5.1.1 Combined Model

A tyre model is developed that encompasses the physical understanding of influence of parameters like tyre size, inflation pressure etc. on tyre rolling resistance coefficient. The exercise is a rather simple assumption of rolling resistance phenomena as stated in section 3.1 and does not account for the complete material behaviour.

The combined model is a result of many layers of mathematical modelling. It starts with the basic assumption of a linear spring and damper model. The lumped damping model includes coulomb damping to explain the velocity dependence at low values. Further, there is inclusion of tyre geometry and material behaviour in the constant belt model. Rotational aerodynamic drag is a further addition to explaining the behaviour of the RRC at high velocity. The results obtained from the combined model are compared to experimental data in [6], to estimate the ability of the model in explaining tyre rolling resistance phenomena. After tuning the damping coefficients for velocity dependence with experimental data from LeanNova (Figure 7.4, Appendix I), the influence of tyre parameters are assessed. In comparing the results, a tyre of size 175/70 R14 was assumed for the default test condition of 2.1 bars, 80% of maximum load capacity, velocity of 80 km/h.

- It is observed that for a decrease of inflation pressure by 14.3%, from 2.1 bars to 1.8 bars, the RRC value increased by 5.6%. The experimental data suggest an increase in RRC value by 6%, for the same changes and the test condition. The result from combined model is in good agreement with the trend observed from experimental data.
- It is observed that for an increase in tyre diameter by 8.3%, the RRC value decreased by 4.84%. The experimental data suggest a decrease in RRC value by 5%, for the same changes and the test condition. The result from combined model is in good agreement with the trend observed from experimental data.
- It is observed that for a decrease in contact patch width (roughly assumed as tyre width) by 50% at 50 km/h, from 280mm to 140mm, the RRC value increased only by 10.4%. The experimental data in [19] for truck tyre suggests a flat plot for a similar tyre width change and velocity, indicating a rather moderate influence. An exact comparison of tyre width influence could not be made, since the experimental plot of passenger car tyres for the parameter could not be found. However, it gives an idea that the influence is rather moderate, which is referred to in section 2.2.1.

- It is observed that for an increase in normal load, from 80 to 90 % of the maximum tyre loading at aforementioned test condition, the RRC value decreased by 6.5%. The experimental data suggest a decrease in RRC value by 3%, for the same changes and the test condition. Clearly the combined model overestimates the normal load influence on RRC. The contribution of temperature to viscoelasticity [6], the width dependence of coulomb damping and influence of complete material behaviour is not explained by the combined model.

A sensitivity analysis of the parameters' influence from table 6 in section 4.6 suggests that change in tyre inflation pressure has the maximum influence on rolling resistance while outer diameter is the most sensitive parameter. The influence of contact patch width is very moderate.

### 5.1.2 Energy simulations

The energy simulation tool from LeanNova was used as a platform for directly comprehending the influence of various parameters in terms of average fuel or energy consumption, from a high to low rolling resistance setting. The overall influence of all the parameters from a nominal to low rolling resistance setting was also obtained for conventional vehicles and pure electric vehicle in NEDC mode.

- It was observed that changing the tyre parameter from nominal to low rolling resistance setting translates to a reduction of 1.3% in average fuel consumption.
- It was observed that changing the tyre parameter from nominal to low rolling resistance setting in pure electric vehicle mode translated to a reduction of 3.8% in average energy consumption.
- For a change in inflation pressure from high to low rolling resistance (1.8 to 3 bars), which is a 66.7 % increase, the average energy consumption for electric vehicle decreased by 4.6%.
- For a change in tyre outer radius from high to low rolling resistance (0.28 to 0.33m), which is a 17.9 % increase, the average energy consumption for electric vehicle decreased by 0.011%. The consumption decrease appears to be an inconsistent indication of the influence of tyre radius when compared to the combined model. The corresponding value of conventional vehicle mode in the energy simulation yields 0.5% decrease in average fuel consumption.
- For a change in inflation pressure from high to low rolling resistance (0.155 to 0.235m), which is a 51.6 % increase, the average energy consumption for electric vehicle decreased by 1.4%.

## 5.2 Future Work

This thesis work is a study initiated to understand the physical influence of operational parameters on tyre rolling resistance. However, the model has potential to develop in its present form. The possibility of testing a tyre that is being considered in vertical stiffness calculations can yield exact constants that shall take into account tyre geometry and material property for the specific tyre. The damping model in the study has been lumped in terms of sidewall shear and radial transition at contact patch edges and instead may be delved deeper by looking at models allowing for tread and sidewall motion in different directions. Effect of temperature can be significant on viscoelasticity and inflation pressure, which may be included in the combined model. The effect of rotational aerodynamic drag can be improved by considering data for drag coefficient and tyre tread geometry. Secondary effect like tyre longitudinal slip which was stated as a stretched target in the thesis work, can account for dynamic cases of tyre deformation behaviour. It can impact energy consumption by changing the offset 'e' in rolling resistance phenomena and by speed losses which would require more energy from vehicle prime mover and hence can be thought of investigating.

## 6 References

- [1] Epa.gov, (2014). *Sources / Climate Change / US EPA*. [online] Available at: <http://www.epa.gov/climatechange/ghgemissions/sources.html> [Accessed 6 Jun. 2014].
- [2] Global.yokohamatire.net, (2014). *Rolling Resistance and Fuel Consumption / TIRE CARE & SAFETY / THE YOKOHAMA RUBBER CO.,LTD..* [online] Available at: [http://global.yokohamatire.net/technology/tirecareandsafety/rolling\\_resistance.html](http://global.yokohamatire.net/technology/tirecareandsafety/rolling_resistance.html) [Accessed 6 Jun. 2014].
- [3] Anon, (2014). 1st ed. [ebook] Available at: [https://www.conti-online.com/generator/www/au/en/continental/tyres/general/downloads/download/reifengrundlagen\\_en.pdf](https://www.conti-online.com/generator/www/au/en/continental/tyres/general/downloads/download/reifengrundlagen_en.pdf) [Accessed 6 Jun. 2014].
- [4] The-contact-patch.com, (2014). *Book : The Contact Patch*. [online] Available at: <http://the-contact-patch.com/book/road/c1610-rubber-tyres> [Accessed 6 Jun. 2014].
- [5] Ordertyres.com, (2014). *Glanworth Tyres*. [online] Available at: <http://www.ordertyres.com/default.asp?action=tyres> [Accessed 6 Jun. 2014].
- [6] Anon, (2014). 1st ed. [ebook] Available at: [http://automotive.ing.unibs.it/~gadola/Michelin/Resistance\\_UK.pdf](http://automotive.ing.unibs.it/~gadola/Michelin/Resistance_UK.pdf) [Accessed 6 Jun. 2014].
- [7] Sandberg, U., Haider, M., Conter, M., Goubert, L., Bergiers, A., Glaeser, K., Schwalbe, G., Zöller, M., Boujard, O., Hammarström, U., Karlsson, R., Ejsmont, J., Wang, T. and Harvey, J. (2011). *Rolling Resistance – Basic Information and State-of-the-Art on Measurement methods*. SP 1 Measurement methods and source models.
- [8] Segel, L. and Xiao-Pei, L. (1982). Vehicular resistance to motion as influenced by road roughness and highway alignment. *Australian Road Research*, 12(4).
- [9] Grover, P. (1998). Modeling of Rolling Resistance Test Data. [online] Available at: <http://dx.doi.org/10.4271/980251> [Accessed 6 Jun. 2014].
- [10] Wong, J. (1978). *Theory of ground vehicles*. 1st ed. New York: Wiley.
- [11] Thompson, G. and Torres, M. (1977). Variations in tire rolling resistance.
- [12] A handbook for the rolling resistance of pneumatic tires Clark, Samuel Kelly;



Dodge, Richard N. 1979

- [13] Clark, S. (1977). Geometric effects on the rolling resistance of pneumatic tyres.  
In: *Tire rolling losses and fuel economy*.
- [14] Hunt, J., Walter, J. and Hall, G. (1997). The effect of tread polymer variations on radial tire rolling resistance. In: *Tire rolling losses and fuel economy*.
- [15] Grappe, F., Candau, R., Barbier, B., Hoffman, M., Belli, A. and Rouillon, J. (1999). Influence of tyre pressure and vertical load on coefficient of rolling resistance and simulated cycling performance. *Ergonomics*, 42(10), pp.1361--1371.
- [16] Nielsen, L. and Sandberg, T. (2002). A New Model for Rolling Resistance of Pneumatic Tires. [online] Available at: <http://dx.doi.org/10.4271/2002-01-1200> [Accessed 6 Jun. 2014].
- [17] Rhyne, T. B. "Development of a Vertical Stiffness Relationship for Belted Radial Tires," *Tire Science and Technology*, TSTCA, Vol. 33, no. 3, July-September 2005, pp. 136-155.
- [18] Wikipedia, (2014). *Drag (physics)*. [online] Available at: [http://en.wikipedia.org/wiki/Drag\\_\(physics\)](http://en.wikipedia.org/wiki/Drag_(physics)) [Accessed 6 Jun. 2014].
- [19] Ali, R., Dhillon, R., El--Gindy, M., "Oijer, F., Johanson, I. and Trivedi, M. (2013). Prediction of rolling resistance and steering characteristics using finite element analysis truck tyre model. *International Journal of Vehicle Systems Modelling and Testing*, 8(2), pp.179--201.
- [20] Varghese, A. (2013). *Influence of Tyre Inflation Pressure on Fuel Consumption, Vehicle Handling and Ride Quality*. Chalmers University of Technology.

# Appendix I

Matlab code for the combined model:

```
function [e,RRC,RR] = TyreModel(R,Vx,N,W,P)

% Input parameter units
% % N = 5000;      %% Normal Load (Newtons)
% % W = 0.165;     %% Section Width (Metres)
% % P = 250000;    %% Inflation Pressure (Pascal)
% % Ro = 0.5612/2; %% Tyre Outer Diameter (Metres)
% % Vx = 80*5/18;  %% Longitudinal speed (Metres/Second)

% Constants
n= 500; %% number of divisions of contact patch
Cv = 0.5/n; % Viscous Damping coefficient
Cc = 180/n; % Coulumb Damping/Friction damping coefficient
Cd = 1/280; % some kind of Rotational drag constant (skin friction + form drag)

%% Calculation of contact patch lenght L
Kz =(0.0274*(P/100000)*sqrt(2e+6*(W*0.7)*R) +3.38)*10000;
delta_z = N./Kz;
a=R-delta_z;
theta_max = acos(a/R); %% maximum angle corresponding to contact patch
w = Vx/R;      %% Angular Velocity
theta = -theta_max;

fx=0;
f=0;

%% vertical calculations
i = (2*theta_max)/n; %% Longitudinal Resolution in contact patch

for Ita = 1:n+1
z = -R*(cos(theta) - cos(theta_max)); %% Vertical deformation of 'i'th element
dz = -w*R*sin(theta); %% Rate of vertical deformation of 'i'th element
Fz = -(Cv*dz+ Cc*sign(dz) ); % Normal Force at 'i'th element due to damping
x=a*tan(theta);
```

```

%% For calculation of e, where  $e = (\text{integration of } F_z * x * dx) / (\text{integration of } F_z * dx)$ 
fx = fx + Fz*x; %% (integration of  $F_z * x * dx$ )
f= f + Fz; %% (integration of  $F_z * dx$  without the normal load component due to
pressure)
theta = theta + i;
end

%% Final calculations for output of the model

fx = fx + (Vx^2)*(W*2*pi*R)*Cd; %% 2nd degree velocity dependence due to
rotational aerodynamic drag
f=f + N; %% f = Normal Load ( $f=0 + N$ )
e = (fx/f);
RRC= e/R; %% Rolling resistance coefficient calculation
RR= RRC*N;
end

```

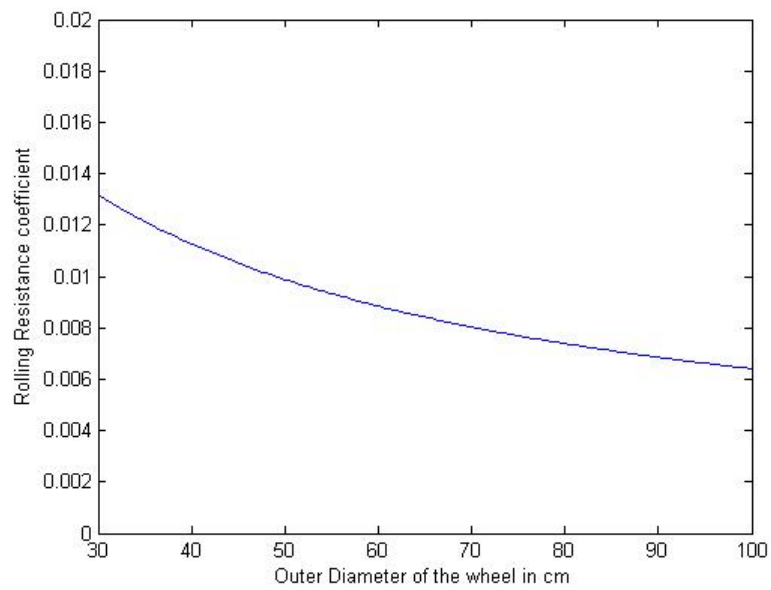


**Figure 7.1 RRC vs Tyre outer diameter for 175/70 R14,  $P = 2.1$  bar, 80 % Max Load,  $V = 80$  km/h (combined model)**

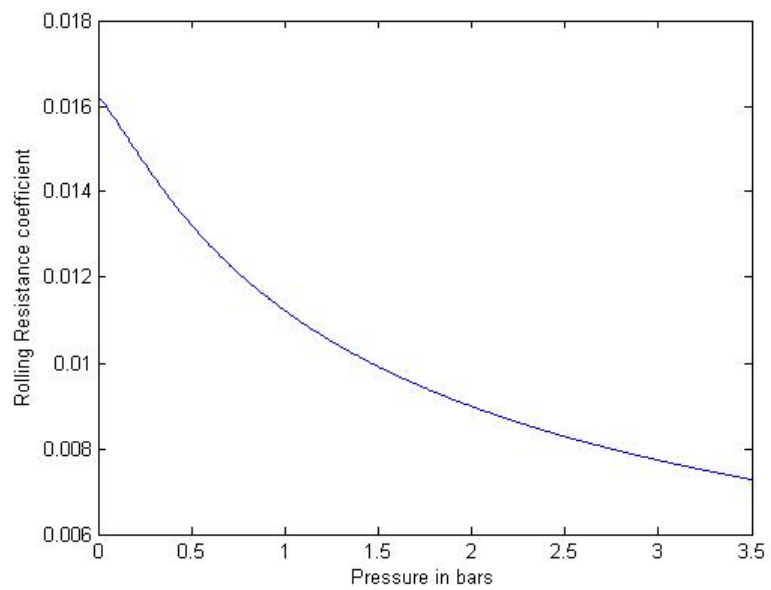


**Figure 7.2 RRC vs Tyre inflation pressure for 175/70 R14,  $V = 80$  km/h, 80 % Max Load (combined model)**

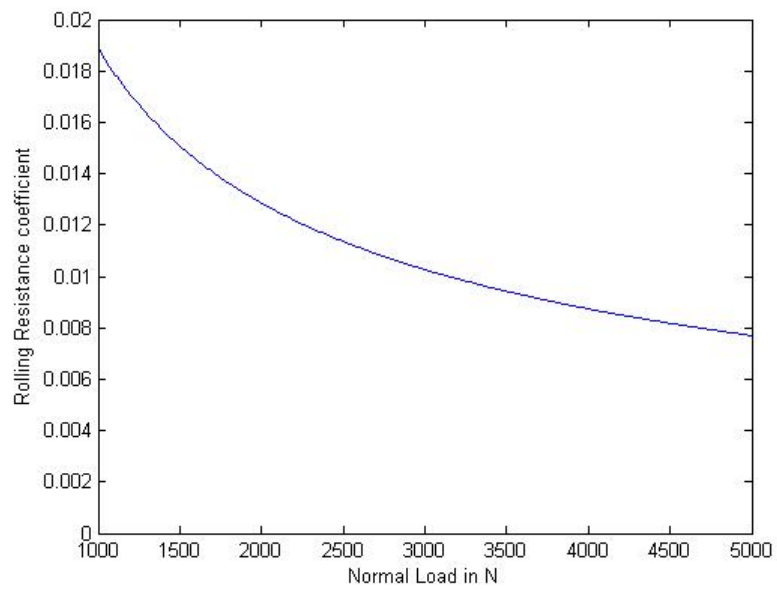


Figure 7.3 RRC vs normal load for 175/70 R14, P = 2.1 bar, V = 80 km/h (combined model)

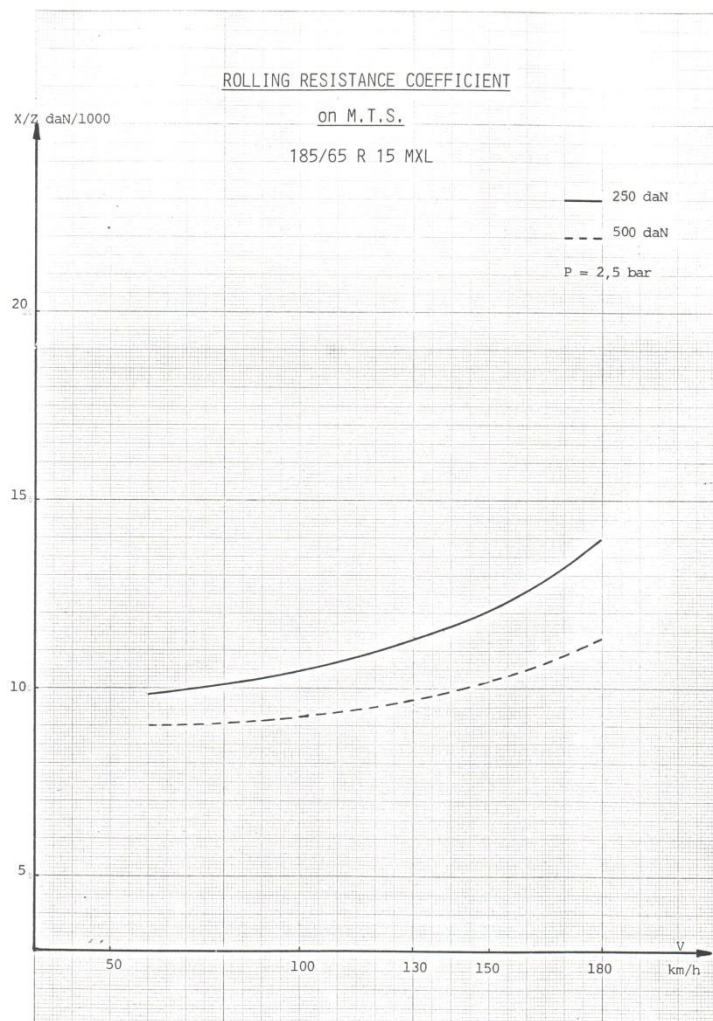


Figure 7.4 RRC vs normal load for 175/70 R14, P = 2.1 bar, V = 80 km/h from LeanNova